Mass spectrometry advances in analysis of glioblastoma

Sofian Al Shboul[1], Ashita Singh[2], Renata Kobetic[3], David R. Goodlett[4], Paul M Brennan[5], Ted Hupp[2], Irena Dapic[3*]

[1]Department of Pharmacology and Public Health, Faculty of Medicine, The Hashemite University, Zarqa, 13133, Jordan

[2]Institute of Genetics and Cancer, University of Edinburgh, Edinburgh, Scotland, UK

[3]Ruder Boskovic Institute, Bijenicka cesta 54, 10 000 Zagreb, Croatia

[4]University of Victoria-Genome BC Proteomics Centre, Victoria, British Columbia V8Z 7X8, Canada

[5]Translational Neurosurgery, Centre for clinical brain sciences, University of Edinburgh, Edinburgh, United Kingdom

*Corresponding author:

idapic@irb.hr, Ruder Boskovic Institute, Zagreb, Croatia; tel: +385 91 545 2328

Running head: Mass spectrometry in glioblastoma analysis

[22

Abstract

Some cancers such as glioblastoma (GBM), show minimal response to medical interventions, often only capable of mitigating tumour growth or alleviating symptoms. High metabolic activity in the tumour microenvironment marked by immune responses and hypoxia, is a crucial factor driving tumour progression. The many developments in mass spectrometry (MS) over the last decades have provided a pivotal tool for studying proteins, along with their posttranslational modifications. It is known that the proteomic landscape of GBM comprises a wide range of proteins involved in cell proliferation, survival, migration, and immune evasion. Combination of mass spectrometry imaging and microscopy has potential to reveal the spatial and molecular characteristics of pathological tissue sections. Moreover, integration of MS in the surgical process in form of techniques such as DESI-MS or rapid evaporative ionization MS has been shown as an effective tool for rapid measurement of metabolite profiles, providing detailed information within seconds. In immunotherapy-related research, MS plays an indispensable role in detection and targeting of cancer antigens which serve as a base for antigen-specific therapies. In this review, we aim to provide detailed information on molecular profile in GBM and to discuss recent MS advances and their clinical benefits for targeting this aggressive disease.

Keywords: glioblastoma, mass spectrometry, proteomics, lipids, glycans, tissues

Table of Contents

1. Introduction

1.1. Overview of GBM (diagnostics and the current treatment options)

Glioblastoma (GBM) is a highly malignant heterogeneous brain tumour with a high rate of therapeutic resistance and recurrence (Hanif et al., 2017). The current management approach typically involves tumour debulking followed by intensive radiotherapy and temozolomide (TMZ) -based chemotherapy. However, the inability to achieve complete tumour resection, coupled with the significant side effects of radiation and TMZ, ultimately constrains their clinical efficacy (Davis, 2016; Lee and Wee, 2022). Despite these treatment modalities, the prognosis remains grim for most GBM patients, particularly isocitrate dehydrogenase-1 (IDH1)-wildtype, as they typically succumb to death within 15 months of their initial diagnosis (Tan et al., 2020).

1.2. Genetic and Molecular Characteristics of GBM (2021 classification)

Clinically, the WHO 4th edition (2016) incorporated molecular markers into GBM subgrouping according to their IDH1 status, which has been shown to better correlate with tumour biology and patient prognosis than the previous purely histology-based classification system (Louis et al., 2016). Moreover, large-scale genomic and molecular analyses of GBM tissues revealed key markers that can be used to suggest comprehensive molecular and clinical classification of high-grade gliomas (Zacher et al., 2017). Genomic events such as TERT promoter mutation, epidermal growth factor receptor (EGFR) gene amplification, +7/-10 chromosome copy number changes and deletion of CDKN2A/B were indeed incorporated in the latest WHO central nervous system (CNS) tumours classification (5th edition/2021) (Louis et al., 2021). Accordingly, GBM is defined as an adult grade 4 diffuse astrocytic glioma IDH-wildtype and has one of the following genetic parameters: TERT promoter mutation, EGFR amplification, chromosome 7 gain/loss and chromosome 10 loss/gain or CDKN2A/B deletion (Louis et al., 2021). Grade 4 astrocytoma can be diagnosed based on a molecular signature (any of the previously mentioned events), even in the absence of malignant histological features (Louis et al., 2021). Such an approach emphasises the importance of integrating molecular and genomic data for a comprehensive understanding of gliomas from a clinical point of view.

The 2021 classification primarily emphasized the clinical significance of genomic events in GBM. However, a more comprehensive molecular classification has delineated GBM into four distinct subtypes: proneural, classical, mesenchymal, and neural (Brennan et al., 2013; Zhang et al., 2020). Nonetheless, recent studies have raised concerns about potential misclassification associated with the neural subtype, particularly in samples containing a substantial proportion of normal tissue (Madurga et al., 2021). These GBM subtypes showcase unique genetic and molecular characteristics, holding substantial relevance for patient management strategies and the selection of appropriate treatments.

The proneural subtype is characterized by the expression of genes involved in neurogenesis, such as PDGFRA, OLIG2, and SOX2 (Brennan et al., 2013; Cancer Genome Atlas Research, 2008; Verhaak et al., 2010). The classical subtype is defined by the overexpression of genes such as EGFR, AKT2, and NOTCH3, which are involved in cell proliferation and growth (Brennan et al., 2013; Cancer Genome Atlas Research, 2008; Verhaak et al., 2010). The mesenchymal subtype is associated with genes related to angiogenesis and invasion, such as YKL40, MET, and CD44 (Brennan et al., 2013; Cancer Genome Atlas Research, 2008; Verhaak et al., 2010). The molecular subtypes of GBM have important clinical implications. For example, the mesenchymal subtype has been associated with a more aggressive phenotype and resistance to standard therapies, while the proneural subtype has been linked to a better response to certain targeted therapies (Brennan et al., 2013; Cancer Genome Atlas Research, 2008; Phillips et al., 2006; Verhaak et al., 2010). Integrating molecular subtyping alongside other clinical and histological features can provide a more comprehensive understanding of GBM and improve patient care strategies.

1.3. Molecular Pathways Implicated in GBM Development and Progression

The advancements in molecular and genomic characterizations of GBM have unveiled pivotal pathways orchestrating tumour growth, invasion, and therapeutic resistance. Among these, the PI3K/AKT/mTOR pathway stands prominently, frequently dysregulated in GBM (Zhang et al., 2020). This pathway crucially fosters cell survival, proliferation, and growth. Genetic alterations like Phosphatase and Tensin Homolog (PTEN) loss and phosphatidylinositol 3-kinase (PI3K) mutations lead to its hyperactivation, significantly contributing to the aggressive nature of GBM (Wang et al., 2021b). Additionally, the EGFR pathway emerges as another cornerstone in GBM pathogenesis (Oprita et al., 2021). EGFR

amplification and mutation, common in GBM, perpetuate continuous downstream signalling pivotal in cell proliferation, survival, and invasion. Notably, the mutated EGFRvIII variant correlates with an intensified GBM phenotype (Oprita et al., 2021). Furthermore, mutations compromising the p53 gene function critically undermine its role in regulating cell cycle arrest, DNA repair, and apoptosis. This malfunction significantly fuels uncontrolled cell division and genomic instability in GBM (Grochans et al., 2022). The most prominent deletion identified is within the CDKN2A/B gene region, observed in approximately 50% of GBM tumours. Additionally, the adjacent IFNA locus is co-deleted in around 25% of GBM patients, marking one of the highest frequencies of IFNA deletion observed in any human tumour type (Al Shboul et al., 2024). These findings imply a significant immunological aspect in the evolution of a subset of GBM. In addition, extrachromosomal DNA (ecDNA) has been observed to harbour key oncogenes such as EGFR and Platelet-Derived Growth Factor Receptor Alpha (PDGFRA), both of which are frequently amplified in this aggressive brain tumour (Purshouse et al., 2022). The presence of ecDNA carrying these oncogenes can lead to their overexpression, driving tumour growth and progression. One significant aspect of ecDNA is its ability to undergo dynamic changes in copy number, facilitating the rapid adaptation of cancer cells to changing environmental conditions, including exposure to therapeutic agents (Lange et al., 2022). This adaptability can contribute to treatment resistance, as cells harbouring ecDNA may survive and proliferate despite targeted therapies aimed at inhibiting the amplified oncogenes. Understanding these pathways not only sheds light on the molecular underpinnings of GBM but also underscores their clinical significance. Their dysregulation is intricately linked to GBM's aggressive behaviour, therapy resistance, and rapid progression, underscoring their relevance as potential therapeutic targets.

One major issue lies in the inherent genetic and molecular heterogeneity of GBM, which makes it challenging to identify uniform biomarkers that can accurately classify and predict patient outcomes. For example, with respect to CDKN2A/B locus, wild type, homozygous deletion and even tetraploid (amplification) populations can be seen in the same field (Al Shboul et al., 2024). GBM molecular classifications might not fully capture the dynamic changes that occur in tumours over time or in response to treatment and the heterogeneity within these subtypes still presents a challenge in identifying targeted therapies (Brennan et al., 2013; Cancer Genome Atlas Research, 2008). Further

limitation comes from the lack of standardized methodologies and databases for the collection and analysis of molecular and genomic data. The integration of such data requires consistent and reliable methodologies, as well as a comprehensive database for the storage and analysis of this data. The absence of such standardization can lead to inconsistencies in the interpretation of results and limit the development of precision medicine approaches for GBM treatment (Nørøxe et al., 2020).

1.4. Experimental models to study GBM

Another major issue is the limitation of the *in vitro* (two-and three-dimensional) cell culture models as well as *in vivo* animal models in accurately replicating the complexity of GBM within the human brain. In addition, these models fail to address tumour heterogeneity and plasticity of tumour-initiating stem cell lineages, which are the primary source of resistance and recurrence (Auffinger et al., 2015). Utilizing patient-derived cancer stem cells can partially mitigate these challenges. These models can closely mimic the features of patient tumours, particularly genetic background, providing a more accurate representation of pathobiology and drug responses compared to conventional cell lines. Furthermore, they can effectively capture the heterogeneity present in patient tumours, facilitating personalized medicine approaches that could result in more precise and effective treatment strategies (Boccellato and Rehm, 2022). Moreover, they offer valuable insights into the mechanisms of drug resistance and tumour recurrence, aiding in the development of strategies to overcome treatment resistance and enhance patient outcomes. However, *in vitro* cell cultures still fail to replicate the intricate tumour microenvironment (TME), which significantly influences tumour behaviour and response to therapy. Moreover, it is widely acknowledged that *in vitro* modelling comes with significant limitations, such as the absence of interactions with other cell types, the lack of influence from cytokines and other cell signalling molecules, and the loss of tumour tissue architecture (Mirabelli et al., 2019).

Mouse models provide valuable insights into tumour cell interactions within the brain environment, blood-brain barrier drug penetration, and drug efficacy. Patient-derived xenograft (PDX) models involve implanting fresh human tumour tissue into a mouse brain. However, PDX models can only be established in immunodeficient mice to prevent rejection of human tissue, which compromises the critical roles of immune cells in tumour biology (Liu et al., 2024). Notably, drugs deemed effective in

mouse models have consistently failed in clinical trials, highlighting the need for more robust model to accurately predict clinical efficacy (Bausart et al., 2022).

Lately, there has been a resurgence of interest in the use of patient-derived tissue slice culture models, particularly in the context of brain tissue and GBM. This approach provides *ex vivo* access to brain tissue architecture, while also more effectively recapitulating tumour heterogeneity, cellular complexity, and the TME, enabling monitoring of live cell behaviour across multiple lineages, including response to drugs (Minami et al., 2017). It enables tractable modelling of both the invasive tumour edge and hypoxic tumour core. The tumour tissue discarded during surgery can be used to make, 250-300 µm tissue slices that can be cultured above a semipermeable membrane in a cell culture insert and exposed to medium supplemented with serum. These cultures retain viable, metabolically active cells for up to 14 days. Slice cultures have been utilized to explore mechanisms underlying tumour cell infiltration and migration by assessing the response of glioma cells to brain tissue (Matsumura et al., 2000). Utilizing proteomics analysis on such clinically relevant models should provide a better window into the biochemistry of tumour cells, which in turn can uncover critical molecular pathways involved in tumour progression and therapeutic response, possibly leading to the development of more effective treatment strategies for GBM patients.

GBM organoids, which are 3D self-organized neural tissue that display brain-like architecture, have emerged as powerful experimental models to study GBM biology and evaluating therapeutic approaches. These organoids can be generated directly from tumour cells obtained from GBM patients or can be co-cultured with immune cells, endothelial cells, and astrocytes to recapitulate key features of the TME, and cellular heterogeneity found in GBM tumours in vivo (Rybin et al., 2021; Zhang et al., 2020). Proteomic analysis of GBM organoids using MS offers an unbiased, systems-level view of the proteins and pathways driving these aggressive tumours (Fan et al., 2024; Wang et al., 2024). A recent multidimensional atlas of human GBM-like organoids integrated proteomic and phosphoproteomic data with genomic, transcriptomic, metabolomic and lipidomic analyses revealed that genetic heterogeneity affects multiple molecular layers in GBM organoids and identified potential targets and pathways for genotype-based treatment (Wang et al., 2024). Additionally, Schuster et al., analyzed media from cultured organoids and extracellular vesicle (EVs) by high-resolution MS and found that EVs from 3D

organoids were enriched for immune regulatory signalling biomolecules and contained an altered miRNA and protein cargo associated with tumour progression and immunosuppression. This suggests that 3D GBM organoids may provide a more clinically relevant model for studying how tumour-derived EVs modulate the surrounding microenvironment (Schuster et al., 2024). Despite their potential, there are currently a limited number of studies applying MS-based proteomics to analyze these cell culture systems. As MS technologies continue to advance, more studies are expected to leverage proteomics to interrogate the complex biology of GBM organoids and identify novel therapeutic targets and biomarkers.

Proteomics is a well-established set of technologies for studying proteins in complex mixtures such as cells from the TME. As such, proteomics offers a promising avenue to address some of the abovementioned limitations. Unlike genomic analyses, proteomic approaches directly analyze proteins, reflecting the functional status of cells and providing a more dynamic representation of the tumour's biology (Pandey and Mann, 2000). Proteomics can unveil post-translational modifications, protein-protein interactions, and changes in protein expression that might not be evident at the genomic level. This depth of information can offer a more comprehensive understanding of the tumour's behaviour, including its response to therapy and potential mechanisms of resistance. Additionally, proteomic analyses can capture the tumour's adaptive changes, potentially identifying subpopulations of cells that evolve under treatment pressures, guiding more tailored and effective therapies (Kwon et al., 2021). Furthermore, the integration of proteomic data with genomic and molecular information can offer a more holistic view of GBM, overcoming some of the limitations associated with singular molecular classifications. There is a range of mass spectrometry techniques (Scheme 1.) used to analyse content of GBM cells, all with the aim to better understand progression and find a cure for treatment of GBM. This review will discuss the recent advancements in mass spectrometry-based proteomic approaches and the various approaches to analyze patient's tumour tissues to gain insights into the intricate molecular landscape of GBM.

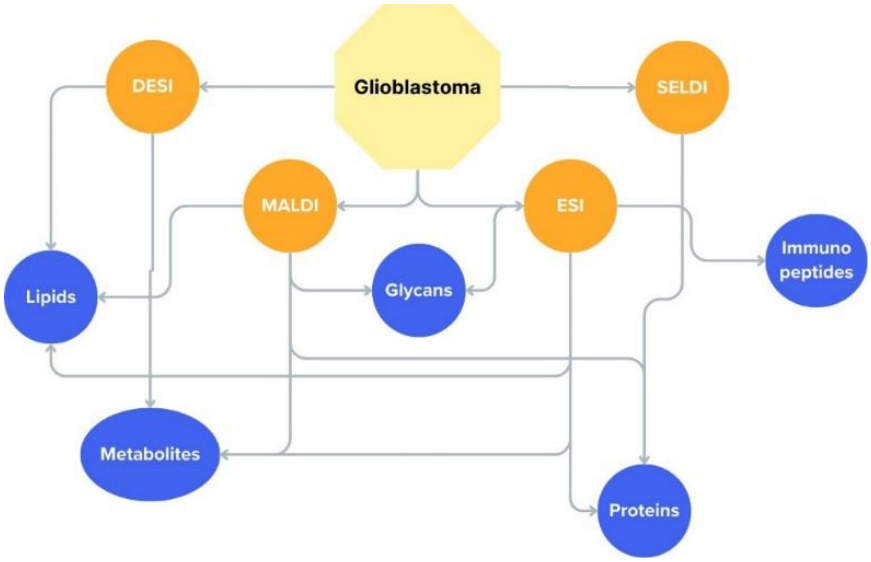

Scheme 1. Illustration of mass spectrometry based techniques used in the analysis of different classes of molecules in the studies of glioblastoma. Electrospray ionization (ESI); Desorption electrospray ionization (DESI); Matrix-assisted laser desorption/ionization (MALDI); Surface-enhanced laser desorption/ionization (SELDI).

2. Tumour microenvironment (TME) in GBM

The GBM TME is a dynamic setting where a variety of cell types, including cancer and cancer stem cells, immune and inflammatory cells, cancer-associated fibroblasts (CAFs), tumour-associated macrophages (TAMs), adipose cells, and endothelial cells, engage in continuous interactions (Schmassmann et al., 2023). While these cells perform diverse functions, the primary outcome of their interactions is to support tumour survival and progression, therefore, understanding the precise components of TME and their specific roles is a ‘must’ for us to eliminate GBM or, at the very least, impede its progression (Binder and O'Rourke, 2022; Hu et al., 2023). Furthermore, TME is basically a dynamic environment that is heavily influenced by cell-to-cell contact, cellular metabolic products, and non-cell autonomous interactions (Baghban et al., 2020; Dapash et al., 2021). TME is characterized by immunological response and hypoxia, which lately has been described as one of the most important factors contributing to tumoural progression (Wang et al., 2020). In this scenario, cancer cells may engage in competition for nutrients with neighbouring cells, prompting these cells to undergo metabolic remodelling to some extent to fulfil their requirements, ultimately, fostering metastasis and invasiveness

(Sohrabi et al., 2023). Additionally, the metabolic activity of GBM tumour cells may vary among the same tumour due to the heterogeneity of the neo-angiogenesis and the vascular network in GBM (Sharma et al., 2023); such inter- and intra-tumoral variances in vascularization have effects on oxygen disturbance within tumour, which in turn can influence the metabolic properties and energy utilization of tumour cells (Giles et al., 2023). Therefore, tumour cells within the same tumour can have differential metabolic signatures. It is well known that GBM cells undergo significant alterations in their metabolism to support rapid growth and adapt to the hostile environment of the brain (Shakya et al., 2021). These changes are driven by various genetic mutations, such as those in the IDH gene, amplification of EGFR, loss of PTEN, and O-6-methylguanine-DNA methyltransferase (MGMT) promoter mutation, resulting in a metabolic phenotype that favours cancer cell survival and proliferation (Duan et al., 2015; El Khayari et al., 2022; Munoz-Hidalgo et al., 2020; Yan et al., 2009). Another prominent metabolic adaptation in GBM is the upregulation of aerobic glycolysis, also known as the Warburg effect, whereby cancer cells preferentially metabolize glucose to lactate even in the presence of oxygen (Liberti and Locasale, 2016; Stanke et al., 2021; Vander Heiden et al., 2009). This metabolic shift not only provides GBM cells with a rapid source of energy but also generates metabolic by-products that can modulate the TME, including lactate-mediated immunosuppression and acidification of the extracellular milieu. Furthermore, the metabolism of lipids has a key role in sustaining the rapid proliferation of GBM cells by providing structural components for membrane synthesis and serving as a reservoir for bioenergetic intermediates (Choo et al., 2023). Dysregulated lipid metabolism in GBM contributes to the accumulation of lipid droplets and alterations in fatty acid composition, which can impact tumour cell proliferation, migration, and therapy resistance (Kao et al., 2023).

3. LC-MS in the detection of proteins in GBM

Identification of proteins using MS stands as the paramount technique for determining protein levels and exploring potential biomarkers in GBM. MS-based proteomics generally comprised separations of peptides on a reversed phase LC column that is coupled to a tandem mass spectrometer by electrospray ionization (ESI). Presently, the advancement of more efficient MS profiling methods, such as data-independent acquisition (DIA), has demonstrated notable precision and reproducibility in quantifying

mixtures of proteins (Collins et al., 2017). Relevant proteins associated with GBM, including vimentin (VIM) and glial fibrillary acidic protein (GFAP), which are co-expressed in human glioma and linked to the poor survival of GBM patients, have been identified in our study and others (Collins et al., 2017; Weke et al., 2022). Furthermore, there have been identified several immune-related proteins like macrophage migration inhibitory factor (MIF), CD47, and Tweety homolog 1 (TTYH1), which are currently under investigation as targets for immune-related therapies.

The use of primary patient's materials, such as fresh frozen (FF) and formalin-fixed paraffin-embedded (FFPE) tissues, has been instrumental in enabling a detailed analysis of the protein landscape within tumours. FFPE samples are now more accessible for proteomic studies due to improved extraction and MS techniques (Macklin et al., 2020; Weke et al., 2022). This resulted in solidifying their significance in biomarker discovery and understanding cancer pathophysiology. Although FF tissues provide possibly a less altered proteomic profile, they are not as readily available as FFPE, making the latter preferred for extensive analysis for the identification of therapeutic targets and tumour heterogeneity (Azimzadeh et al., 2015; Dapic et al., 2022). However, preservation of the tissue's proteome dynamics is critical from the time of surgical resection to the protein digestion stage, and the extent of how these effects the proteome is poorly understood. This is important since tumour removal surgeries could possibly take hours to finish allowing the sample to be delivered for fixation and preservation processes. Additionally, some cancers can be sampled through rapid procedures like needle biopsies, but these often provide significantly lower amounts of tissue for proteome analysis. FF tissues are often considered superior in terms of providing a more accurate overview of the protein content and post-translational modifications present within the tissue at the time of collection, this is due to the absence of formalin-induced modifications to proteins (Amarnani et al., 2019; Macklin et al., 2020; Weke et al., 2022). Formalin fixation can cause cross-linking of proteins and nucleic acids, as well as chemical modifications such as methylation and hydrolysis, which can affect the integrity and quality of proteins and peptides extracted from the tissue (Pirog et al., 2021) . This can result in a lower yield of some proteins. For example, 2'-5'-Oligoadenylate Synthase 2 (OAS2) was found to be highly abundant in recurrent samples compared to paired primary GBM tissues through RNA-sequencing and proteomic analysis of FF samples. However, its yield was significantly lower in mass spectrometry analysis of

FFPE tissues (Tatari et al., 2022). Nevertheless, FF samples require harsh storage conditions to prevent degradation and require specific instruments to obtain specimens. FFPE, on the other hand, has been preserved for many years allowing for retrospective studies with extensive clinical follow-up data.

Over the past two decades, advancements in proteomic technologies have significantly mitigated some of the challenges linked with FFPE samples, for example, protein crosslinking caused by formalin fixation that produces crosslinked peptides not present in a standard database. These improvements enabled increased effective protein recovery and analysis and enhanced their utility in biomarker discovery (Gustafsson et al., 2015; Zhu et al., 2019). Moreover, the advent of cutting-edge proteomic techniques, including micro- and nano- liter scale sample preparation, laser capture microdissection (LCM), and integrated proteome analysis devices, has markedly refined the detection thresholds and the efficiency of protein extraction from FFPE tissues (Pujari et al., 2023; Zhu et al., 2019).

Several proteins have been identified as abundant in recurrent GBM compared to primary disease. Stem cell lines derived from such patient samples can provide insights into the role of abundant proteins in tumour recurrence and progression. Immunoprecipitation of endogenously epitope-tagged protein using tag antibodies or antibody-conjugated beads, followed by MS analysis, presents an approach to comprehensively understand the role of proteins implicated in the tumour pathobiology (Hubel et al., 2019). Furthermore, the structure and dynamics of protein complexes, as well as peptides, responsible for tumour recurrence and treatment resistance can be studied using cross-linking MS (Kalathiya et al., 2021). This approach provides insights into the functional roles of proteins and their involvement in biological processes. It enables the study of protein-protein interactions and the elucidation of protein complex architectures at the cellular level (O'Reilly and Rappsilber, 2018). Additionally, it provides information on protein partners of highly polymorphic proteins that are challenging to study using other methods (Singh et al., 2022).

Different protein markers have been reported that are associated with GBM (Table 1). Some of them are VEGF and proteins linked to angiogenesis (such as FGF-b, IGFBP-2, Ang2, EGF, and others), extracellular matrix proteins (such as TSP1/2, TNC, Cyr61/CCN1, OPN, etc.), matrix metalloproteinases (MMP-2, MMP-9, AEG-1), cell line associated proteins (GFAP), macrophage migration inhibitory factor (MIF), and proteins functionally related to GBM (such as DDT, CD74,

CD44, CXCR2, and CXCR4) (Silantyev et al., 2019). Surface Enhanced Laser Desorption Ionization (SELDI)-TOF-MS has been demonstrated as an effective method to identify several novel protein biomarkers of glioma (Liu et al., 2014). Proteins showing significant differential expression in GBM tumours compared to epileptic brain tissue are frequently regarded as GBM-specific biomarkers. These proteins have the potential to serve as therapeutic targets for the development of novel treatments. In one report, samples from GBM and epileptic brain tissue were individually separated by SDS-PAGE using internal DNA markers. Subsequently, in-gel trypsin digestion was performed, and the samples were analyzed in triplicate using nano-liquid chromatography-tandem mass spectrometry (nLC-MS/MS) on a Thermo LTQ Orbitrap Velos instrument (Heroux et al., 2014). Results showed that proteins like Serpin H1 SERPINH1 (SERPH), protein disulfide-isomerase P4HB (PDIA1), ceruloplasmin (CERU), tenascin TNC (TENA), vitronectin (VTNC), apolipoprotein E (APOE), galectin-1 LGALS1 (LEG1), histidine-rich glycoprotein (HRG), and peptidyl-prolyl *cis*-trans isomerase (FKBP5), that are known to be involved in tumour progression, aggressiveness, and invasion in GBM were upregulated. Novel GBM-associated proteins as chloride intracellular channel protein 4 (CLIC4), nucleosome assembly protein 1-like 1 (NP1L1), Ig kappa chain C region (IGKC), transgelin-2 (TAGL2), and tyrosine-protein kinase (YES) have been proposed in order to perform precise quantitative analysis of selected proteins in patient-derived GBM xenografts. In another report, a targeted Selected Reaction Monitoring (SRM) workflow, which is the opposite of discovery proteomics discussed so far was developed for use on a triple quadrupole platform, specifically optimized for GBM xenografts treated with bevacizumab. From an initial 100 candidates, 32 proteins were found responsive to anti-angiogenic therapy, whereas malectin, calnexin, lactate dehydrogenase A (LDHA), IDH were proposed as novel biomarkers (Demeure et al., 2016). An important step in understanding the pathobiology of GBM involves integrating diverse metabolic pathways. This integration aids in drawing conclusions about the interdependence of specific metabolites and tumour progression. In a cohort study of 99 treatment-naive GBMs, 10 data types were integrated to better understand overall disease biology, including the proteome with phosphoproteome, lipidome, metabolome, acetylome, whole genome sequencing, whole exome sequencing, RNA sequencing, microRNA-seq, single nuclei RNA-seq, and DNA methylation arrays (Wang et al., 2021a). Phosphorylation of protein tyrosine phosphatase non-

receptor type 11 (PTPN11) and phospholipase C gamma 1 (PLCG1) were found as potential regulators that may activate oncogenic pathways. These events also represent potential targets for tumours with alterations in EGFR, p53, and retinoblastoma 1 (RB1). Results of RNA and protein expression in bulk tumours reveal distinctions in infiltrating macrophages and the distribution of specific immune cell types among GBM subtypes. The study reported a correlation between H2B acetylation and protein expression linked to immune cell functions in GBM. As compared to other tumour subtypes mesenchymal-like GBMs exhibit significant differences and have distinct characteristics. Djuric et al. performed comparative study of FFPE, FF and patient derived cell culture samples to investigate for protein content between the subgroups (Djuric et al., 2019). The study showed that proteomics analysis of FFPE tissues, with minor adjustments in sample preparation techniques, can generate proteomic datasets using MS that are comparable to those obtained from FF tissue samples.

Moreover, serum reflects the TME and utilizing serum proteins as biomarkers provides a less invasive method for diagnosing and monitoring disease progression. While certain serum biomarkers for GBM, such as chitinase-3-like protein 1 (YKL40) and GFAP, have been previously reported, they have exhibited limitations for clinical use.

DIA involves combining fragment ion spectra from all detected peptides in a sample to create a comprehensive digital record representing the measurable proteome using mass spectrometry (Figure 1). Research indicates that DIA has led to over double the peptide identifications and expanded the dynamic range by an additional magnitude compared to traditional data-dependent acquisition (DDA) techniques (Kelstrup et al., 2018) Once obtained, digital maps of tissue or biofluids can undergo multiple in silico examinations to explore novel biochemical hypotheses or identify clinically significant biomarkers. Additionally, the refinement of mass-to-charge (m/z) windows through computational resources can aid in the identification of specific subsets of proteomes. Together with pathological annotations, comprehensive DIA molecular signature of the tumours might be used to predict treatment responses and patient outcomes more accurately, thus aiding in personalized medicine. Use of DIA is rising in quantitative proteomics (Ludwig et al., 2018; F. Zhang et al., 2020) and so far has successfully been applied to different brain tissue samples (Chang et al., 2014; Koopmans et al., 2018; Lagache et al., 2024). Even though after DIA detection proteins could be identified using different

search engines like DIA-Umpire (Tsou et al., 2015) or Spectronaut (Muntel et al., 2019), often better results and higher coverage of the proteins is obtained if project-specific spectral library is composed (Koopmans et al., 2018).

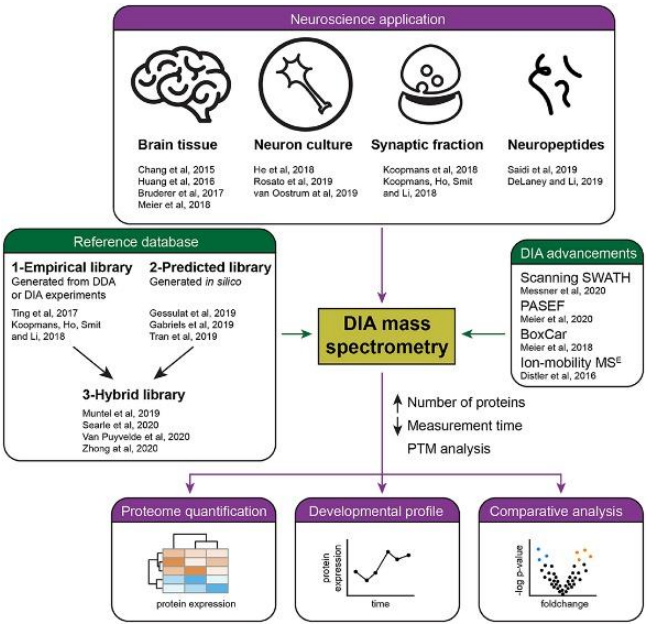

Figure 1. Use of DIA acquisition methods in neuroproteomics. Described studies have used DIA-MS for the quantification of the brain proteome (purple) and advances in DIA which allowed higher throughput and improved databases and libraries (green). Taken and adapted from (Li et al., 2020).

Library usually consists of elution times of identified peptides and their fragments which are further matched with those obtained with DIA. To increase peak capacity and number of proteins identifications ion mobility combined with MSE was applied in profiling of mouse brain proteome in the research of ionizing radiation. (Huang et al., 2016). The combination of IMS-enhanced MSE method and ISOQuant software demonstrated strong reliability and precision, showing minimal median CV values of 0.99% for technical replicates in both the sham and irradiated groups. Biological variability was also minimal, with rates as low as 1.61% for the sham group and 1.31% for the irradiated group. High dynamic range and varying ionization of peptides concentrate the signal within a few peaks instead of distributing it evenly across the mass range. To address this, distributing charge capacity evenly over narrow m/z segments can enhance ion injection times for less abundant species, similar to the approach in DIA methods. This innovative method is called BoxCar method, whereas it optimizes precursor ion

detection by sequentially filling the quadrupole-Orbitrap mass analyzer with different mass windows for improved MS1 performance. BoxCar acquisition method was used on mouse brain tissue and results showed identification of ten thousand protein groups which was 60% more than the analog shotgun–library (Meier et al., 2018). DIA-PASEF (parallel accumulation–serial fragmentation combined with data-independent acquisition) was applied on several GBM studies (Berg et al., 2022; Clavreul et al., 2024; Shen et al., 2024; Y. W. Xu et al., 2021, with the aim to investigate whether PASEF could be used to extend DIA and thus provide more information. DIA-PASEF was used in analysis of 50 FFPE and 31 FF GBM patient samples and tissue sections underwent lipid, protein, and peptide MALDI-MSI examinations. Using unsupervised clustering in MATLAB, distinct spatial patterns for lipid and protein clusters were obtained and results confirmed association of specific lipids and proteins, correlating with patients' diagnosis (Lagache et al., 2024). Moreover, changes in amino acid metabolism within the glioma microenvironment significantly contribute to seizure development. Recent studies have highlighted the impact of protein lysine acetylation on various metabolic processes such as energy metabolism, amino acid metabolism, and fatty acid metabolism. DIA-PASEF was used to investigate role of lysine acetylation in metabolic process of glioma-associated seizures (GAS) (Y. W. Xu et al., 2021). Results showed 407 regulated proteins among which enzymes ACAT2 and ACAA2 were the differentially regulated in the acetylation of GAS. Moreover, increased levels of acetylated proteins were linked with pathways related to the TCA cycle, oxidative phosphorylation, amino acid biosynthesis, and carbon metabolism. Conversely, the decreased acetylated proteins were linked with pathways involving fatty acid metabolism, oxidative phosphorylation, the TCA cycle, and necroptosis. Deregulated acetylation in GBM associated with seizures could be triggered by acetyltransferases, which might be a promising target for therapeutic intervention in managing glioma-related seizures.

With sequential window acquisition of all theoretical fragment ion spectra mass spectrometry (SWATH-MS), which is a data-independent acquisition (DIA) method, eight GBM blood biomarkers candidates were detected, including leucine-rich alpha-2-glycoprotein (LRG1), complement component C9 (C9), C-reactive protein (CRP), alpha-1-antichymotrypsin (SERPINA3), apolipoprotein B-100 (APOB), gelsolin (GSN), Ig alpha-1 chain C region (IGHA1), and apolipoprotein A-IV (APOA4) (Miyauchi et al., 2018). Moreover, the peptide derived from CRP was not detected by a Data dependent

acqusition (DDA) method, which is more stochastic in peptide detection than DIA methods, however it was identified by SWATH-MS using an in-house prepared sequence library. Isobaric Tags for Relative and Absolute Quantitation (iTRAQ) were used to discover and identify biomarker candidates in serum samples, which are considered to reflect the microenvironment of GBM. Two biomarker candidates, S100A8 and S100A9 were further tested in a study of 36 GBM patients and 4 controls, and results showed positive correlation between serum proteins and S100A8 and S100A9 transcripts (Arora et al., 2019). Already in previous studies S100A8 and S100A9 transcripts were found to be significantly higher in mesenchymal GBM subtype, which is enriched with macrophages/microglia infiltration (Wang et al., 2017). Elevated transcripts of S100A8 and S100A9 were indicative of a poor prognosis and only the serum levels of S100A8 demonstrated a correlation with patient survival. Influence of anaesthesia on protein composition was shown in a study involving 34 patients which investigated plasma levels of eight proteins associated with the brain to assess their potential suitability as blood-based biomarkers for malignant gliomas (Lange et al., 2014). The study indicated elevated levels of ICAM-5 and beta-synuclein proteins in gliosarcoma as compared to glioblastoma. Notably, the results showed variations in protein levels between "preanesthetic" and "postanaesthetic" samples of the patients, suggesting that anaesthesia might influence proteins levels and should be taken into consideration when determining biomarkers.

Patterns identified in proteomic and transcriptomic data provide insights into the molecular diversity of GBM tumours, elucidating functionalities associated with patient survival and clarifying the impact of each expression technique. The integrated examination of protein expression and RNA expression yielded findings demonstrating a stronger correlation between survival and proteomic profiles, establishing a distinctive protein-based classification that differs from the established RNA-based classification. In a study involving 87 patients that analyzed both FF and FFPE tissues, findings suggested that shorter survival may be linked to inflammation and glycolytic metabolism. These factors are also associated with tumour growth and aggressiveness in GBM (Yanovich-Arad et al., 2021).

In the quantitative proteomic study of endocytic machinery on glioma biopsies of different grades it was reported that gliomas frequently exhibit a reduction in endocytosis. The downregulation of proteins involved in endocytosis can lead to impaired receptor internalization. The endocytic machinery operates

as a tumour suppressor module, obstructing signal of the abnormal growth factor receptor from the plasma membrane and thereby impeding tumour growth (Buser et al., 2019). Under normal conditions isocitric acid is transformed into α-ketoglutaric acid by IDH1/2 enzyme. The enzymes with mutated isocitrate dehydrogenase IDH1/2 have the capability to transform α-ketoglutarate into 2-hydroxyglutarate (2HG). Approximately 90% of IDH1 mutations involve a G to A transition at the second nucleotide of codon 132, leading to the substitution of arginine with histidine (R132H) (Pusch et al., 2011). Generation of 2HG due to R132H mutations in IDH1 contributes to the process of tumorigenesis and as a consequence hypoxia-related conditions are triggered. Another study showed that the ratio of plasma to urinary 2HG could be used to detect presence of IDH1/2 mutations in glioma patients (Lombardi et al., 2015). The 2HG concentrations were determined using ion-pairing liquid chromatography (Lombardi et al., 2015) and while there was no statistically significant distinction in the plasma levels of 2HG between patients with and without an IDH1 mutation, there was a significant difference in the urine 2HG levels. As knowledge of IDH mutations status is crucial for glioma patients, in the future, this knowledge may pave the way for targeted treatment, such as with R132H-IDH1 inhibitor. Detecting 2HG in frozen sections of brain tumour tissues using matrix-assisted laser desorption ionization - time of flight mass spectrometry (MALDI-TOF) emerged as a quick alternative for LC-MS detection of 2HG levels, requiring minimal sample preparation. However, composition of the matrix is a fundamental parameter in MALDI measurements, and previously 4-maleicanhydridoproton sponge (MAPS) was used for detection of 2HG levels in glioblastoma multiforme (Giampa et al., 2016). Given that 2HG is an acidic and hydrophilic compound, it is necessary to find a foundational matrix that could readily dissolve in polar solutions. In Longuespee et al.'s study, a comparison between MAPS and 1,5-diaminonaphtalene (1,5-DAN) showed that matrix utilizing 1,5-DAN provided a 3-fold higher signal for 2HG compared to MAPS (Longuespee et al., 2018). In another study utilizing MALDI-FTICR, authors showed that the use of 1,5-DAN facilitates the C-terminal fragmentation of proteins via ion source decay (Calligaris et al., 2013).

Cerebrospinal fluid (CSF) can also be used as a source to determine biomarkers of disease. Osteopontin (OPN), which is known as T cell activation gene 1 (Eta-1) and secreted phosphoprotein 1 (SPP1), functions as a significant pleiotropic proinflammatory cytokine and extracellular matrix protein. In a

recent CSF study, it was discovered that full-length OPN (OPN-FL) levels were elevated in CSF samples from all cancer patients. Additionally, levels of thrombin-cleaved OPN (OPN-R) and thrombin/ carboxypeptidase B2 (CPB2)-double-cleaved OPN (OPN-L) were significantly elevated in both GBM and non-GBM gliomas compared to patients with systemic cancer and those without cancer (Yamaguchi et al., 2013).

3.1. Phosphoproteomics in GBM

Protein phosphorylation is one of the key events in pathogenesis of GBM (Bijnsdorp et al., 2021; Guo et al., 2015; Joughin et al., 2009; van Linde et al., 2022). Enrichment of phosphopeptides has been reported with the use of 2D gels and a polyvinylidene fluoride (PVDF) membrane (Guo et al., 2015), immobilized metal affinity chromatography (IMAC) columns (Joughin et al., 2009; Lescarbeau et al., 2016), or metal-oxide affinity chromatography most often titanium dioxide (Kozuka-Hata et al., 2012). In a quantitative study of phosphotyrosine mediated pathways in GBM, LC-MS was coupled with isobaric tags for relative and absolute quantitation (iTRAQ), and phosphopeptides were enriched with the use of anti-phosphotyrosine antibodies followed by IMAC (Lescarbeau et al., 2016). The enriched peptides were analysed on Orbitrap Elite or Q Exactive and results revealed increased levels of oncogenic signals, including phosphorylated ERK, MAPK, PI3K, and PDGFR, in murine tumours compared to normal brain tissue. Moreover, elevated phosphorylation on CDK1 Y15 indicated that treatment with MK-1775, a Wee1 kinase inhibitor, blocked phosphorylation at this site, resulting in mitotic catastrophe characterised by elevated DNA damage and increased apoptosis. Stable isotope labelling with amino acids in cell culture (SILAC) based technology, which incorporates heavy isotopes for quantitation into amino acids during cell growth, has been used with collision-induced dissociation (CID) and high-energy collisional dissociation (HCD) fragmentation and detected over 6000 peptides and identified some novel phosphorylation sites on proteins such as nestin, vimentin or EGF receptor (Kozuka-Hata et al., 2012). A phosphoproteomic study on tyrosine phosphorylation-regulated kinase 1A (DYRK1A) showed that DYRK1A inhibition leads to accumulation of cyclin B and CDK1 (Recasens et al., 2021). Using LC-MS, the detection of posttranslational modifications in plasma of patients revealed a 24% decline in the quantity of ubiquitinated peptides and a 46% decrease in the

count of acetylated peptides, however there was no significant change in number of phosphopeptides in GBM compared to control group (Petushkova et al., 2017). In the study of patient-derived GBM stem cells using SILAC-based labelling, the integration of network analysis with quantitative phosphoproteomics revealed the essential signalling pathways and molecules implicated in the serum-induced changes in glioblastoma stem cells. Peptides analysis on nanoLC-coupled to a LTQ Velos led to identification of 2876 phosphorylation sites corresponding to 1584 proteins which corresponded to 2523 phosphorylated serine (pS), 317 phosphorylated threonine (pT), and 36 phosphorylated tyrosine (pY) residues (Narushima et al., 2016). While most of the studies used DDA for detection of phosphopeptides, a study on an established GBM cell line, U87, utilised parallel reaction monitoring (PRM) for quantitative analysis. Direct-PRM (tryptic digest of all peptides) was compared to the same sample where phosphopeptides were first enriched by TiO2 and then PRM was performed (Dekker et al., 2018). Some proteins such as neuroblast differentiation-associated protein (AHNAK S5480-p), calcium/calmodulin-dependent protein kinase type II subunit delta (CAMK2D T337-p), and EGFR S1166-p, were consistent across two sample preparation methods. However, in U87 cell line deprived of serum, large changes in phosphorylation of EGFR and AHNAK were observed due to the absence of serum (Dekker et al., 2018). PRM monitoring was also employed to identify the phosphoproteome of FFPE and FF GBM tissues. This was done with both, tryptic digest without phosphopeptide enrichment (Direct-PRM) and after Fe-NTA phosphopeptide enrichment (Fe-NTA-PRM) (Zeneyedpour et al., 2020). The detected proteins, including neuroblast differentiation-associated protein (AHNAK) S5448-p, calcium/calmodulin-dependent protein kinase type II subunit delta (CAMK2D) T337-p, eukaryotic translation initiation factor 4B (EIF4B) S93-p, and EGFR S1166-p were quantified with high reproducibility (14%) and therefore, FFPE tissues were found to be appropriate for phosphoproteome detection.

The recently developed single-run phosphoproteomics workflow, EasyPhos technology, which utilizes 96-well plates, was employed to analyse the global phosphoproteomes of EGF-treated glioblastoma cells (Humphrey et al., 2018). EasyPhos omits peptide desalting step and enables the lysis, digestion, and phosphopeptide enrichment steps to be performed in a single tube. Phosphopeptide enrichment is conducted in acidic conditions, typically using buffers containing 6% trifluoroacetic acid (TFA) to

protonate acidic residues like glutamic and aspartic acid. This process helps restrict their interaction with metal oxide affinity chromatography MOAC or immobilized metal affinity chromatography (IMAC) beads, thereby minimizing the capture of non-phosphorylated acidic peptides, which in the mass spectrometer will obscure the signal of the desired, but less abundant, phosphopeptides. Peptide labelling with tandem mass tag (TMT) tags in a study involving primary and recurrent GBM showed no significantly upregulated phosphosites in recurrent GBM, however an individualized approach to patient samples confirmed substantial heterogeneity of GBM. The study identified 15 phosphosites, including 7 phosphoproteins: stathmin (STMN1), cofilin 1 (CFL1), microtubule-associated protein Tau (MAPT), kininogen-1 (KNG1), neurofilament medium polypeptide (NEFM), SWI/SNF-related matrix-associated actin-dependent regulator of chromatin subfamily C member 2 (SMARCC2), and serine/arginine-rich splicing factor 3 (SRSF3)), which were differentially expressed in recurrent GBM (Dekker et al., 2020).

PamStation 12, a microfluidic workstation, was developed as a "functional proteomics" platform for high-throughput screening and analysis in biological research. It profiles the serine/threonine, tyrosine kinases in a two-step biochemical assay. It was reported how this platform identified high kinomic activity, exemplified by Bruton's tyrosine kinase (BTK), within GBM tissue (Ibrahim et al., 2019). Interestingly, BTK was absent in patient-derived GBM stem-like cell lines, indicating potential limitations of cell lines in tumour modelling. It was further demonstrated that BTK was co-expressed with stem cell marker (SRY (sex-determining region Y)-box 2: SOX2) and/or macrophage markers (CD163 and CD68) (Al Shboul et al., 2021) (Figure 2). Such analytical approaches highlight the need for increased reliance on patient tumour tissue/material as the source of cancer research. Additionally, it emphasizes that proteomics, both functional and kinome analysis, can play a pivotal role in drug and biomarker discovery.

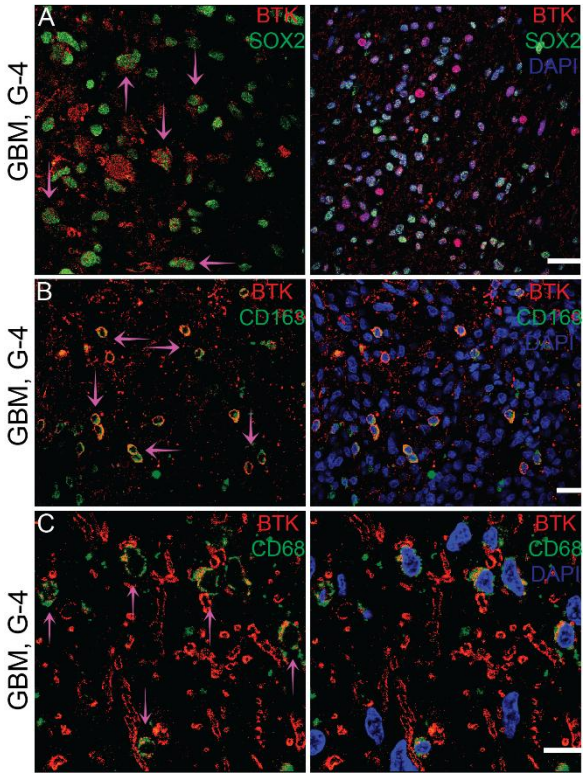

Figure 2. Double immunofluorescence staining of BTK with various biomarkers in GBM FFPE sections. (A) BTK was stained with SOX2, a cancer stem marker. (B) BTK stained with CD163, M2-like macrophage marker. (C) BTK stained with CD68, a pan-macrophage marker. The figure demonstrates that BTK, a tyrosine-protein kinase implicated in blood malignancies was found to be expressed in various cell types (cancer stem cells and/or macrophages) but was notably absent in all GBM cell lines models, as observation in GBM kinome data (Al Shboul et al., 2021). Figure adapted from (Al Shboul et al., 2021).

4. Single cells analysis

Single cells analysis represents an interesting approach to analyse biological samples due to its ability to access cellular heterogeneity and provide additional information about tumours. Different omics approaches including genomics, transcriptomics, metabolomics and proteomics have used single cell analysis in order to improve tissue classification an facilitate biomarkers research (Hu et al., 2023; T. Xu et al., 2022; Yin et al., 2019). However, due to the little cell size, single cell analysis can show large variety in concentrations of low present compounds. Single cell RNA sequencing (scRNA-seq) has emerged as an important approach to reveal complexity which is often contained in complex samples

such as tissues. It has been widely used to investigate intra-tumoural heterogeneity in GBM (Couturier et al., 2020; Patel et al., 2014) and most studies shown complex spatial heterogeneity confirming that samples from different spatial locations were more genetically diverse than locally adjacent tumors (Lee et al., 2017). Mass spectrometry techniques show high sensitivity for single cell detection with advantages such as no need for labelling, low sample consumption, multiplexed detection and high throughput. Integration of multiple analytical modalities such as scRNA-seq and multiplexed tissue imaging gave information about cellular types and states while imaging revealed their spatial location (Coy et al., 2022). Investigation of purinergic signalling showed that pediatric GBM tumours exhibit increased interactions between CD73-expressing tumour cells and CD39-expressing microglia. Results also showed that blocking purine signal might be a used as a immunotherapy for both adult and pediatric HGG (Coy et al., 2022). Recent studies showed that ion channels have an active role in tumour cellular cycle such as differentitation, growth and proliferation. Role of magnesium was studied in F98 rat glioma model with the use of imaging secondary ion mass spectrometry (SIMS) (Chandra et al., 2016). Results showed that normal brain tissue contained significantly lower total Mg concentration as compared to tumour cells (4.70 ± 0.93 mmol/Kg vs 11.64 ± 1.96 mmol/Kg). These findings confirm elevated influx of magnesium into tumour cells and altered Mg homeostasis. Combination of combined droplet extraction and a pulsed direct current electrospray ionization mass spectrometry method (Pico-ESI-MS) was used in the study of metabolites in human astrocyte cells and GBM cells (X. C. Zhang et al., 2018). Results showed more than 300 phospholipids successfully identified from a single cell and that the ratios of unsaturated phosphatidylcholines (PCs) to saturated PCs were significantly higher in GBM cells compared to normal cells. GBM cells also showed presence of a mixture of LPC(17:1) and LPE(20:1) while in astrocyte cells only LPC(17:1) was detected. To investigate for chemotherapeutic drug delivery time of flight secondary ion mass spectrometry (3D-MSI-TOF-SIMS) was used in the study of of A-172 human glioblastoma cell line treated with B-cell lymphoma 2 (Bcl-2) inhibitor ABT-737 (Vanbellingen et al., 2016). Vanbellingen et al. used dual beam analysis with high spatial (~250 nm) and mass resolution (m/Δm ~10 000). Study identified and localized unlabelled drug molecular ion (m/z 811.26 C42H44ClN6O5S2– [M – H]–) and characteristic fragment ions. They proposed semi-

quantitative approach for rapid characterization of multiple single cells while accounting for biological diversity (Vanbellingen et al., 2016).

5. Intraoperative mass spectrometry

Intraoperative MS can give information on tumour pathology and can be used to rapidly detect differences in lipids and oncometabolites in non-malignant adjacent brain and gliomas thus defining tumour margins and type. Intraoperative Desorption electrospray ionization (DESI)-MS was developed with the aim to determine the disease state, specifically identifying glioma, gray matter, white matter, or mixed states, along with estimating tumour cell percentage (TCP) relative to normal cells. DESI involves pointing a stream of electrified liquid at a sample without touching it from which ions are made from those molecules on the surface of the tissue in this case. Since DESI-MS is conducted in an ambient manner with minimal sample pre-treatment there is the possibility of quickly delivering diagnostic information within the operating room (Zhang et al., 2015)**.** To study tumour margins with DESI-MS, 73 biopsies were obtained from 10 surgical resections and results showed that it enables the detection of glioma and the estimation of high tumour cell percentage at surgical margins with a sensitivity of 93% and specificity of 83% (Pirro et al., 2017a). Further DESI-MS showed intraoperative potential in a cohort of 49 patients suspected of having glioma, and was used to determine IDH status, tumour cell percentage and disease status (Brown et al., 2021). DESI-MS successfully detected the IDH-mutation status by measuring the oncometabolite 2-HG in glioma core biopsies, in 51 samples from 25 human subjects. The disruption of isocitrate conversion to α-ketoglutarate, specifically through IDH1 mutations, resulting in elevated 2-HG levels, highlights the potential of this approach for identifying key glioma prognostic markers, particularly R132H mutations, with implications for clinical decision-making (Alfaro et al., 2019). Detection of 2-HG with DESI-MS with high sensitivity and specificity provides rapid diagnostic information about the patient's condition. Integrating the 2-HG signal onto three-dimensional MRI reconstructions of tumours facilitates the fusion of molecular and radiologic information, enhancing clinical decision-making (Figure 3) (Santagata et al., 2014). This method also gives a basis for clinical testing of intraoperative monitoring of tumour metabolites using MS, a development that has the potential to revolutionize how we treat tumours in oncology patients.

Kalinina et al. developed LC-MS method for monitoring of D- and L- forms of 2HG in CSF. Metabolites were derivatized with diacetyl-L-tartaric anhydride (DATAN) and diastereoisomers were detected on AB-Sciex QTRAP 5500 in negative ion mode within 7 minutes (Kalinina et al., 2016). They detected D-2HG threshold of 0.69 μmol/L in CSF, while patients with IDH wild type tumours had levels below, and patients with IDH1/2-mutated tumours had higher levels of 2HG.

Another option to study glioma samples with intraoperative MS involves sampling the tissue using medical swabs. Subsequently, ionization is performed directly from the swab tip after the addition of solvent and application of high voltage (Pirro et al., 2017b). Advantages of this type of analysis are that sampling is minimally invasive, and additional sample pre-treatment is not needed. Touch spray mass spectrometry (TS-MS) serves as a viable alternative when it is not feasible or convenient to position a mass spectrometry instrument in the operating room during the surgical procedure.

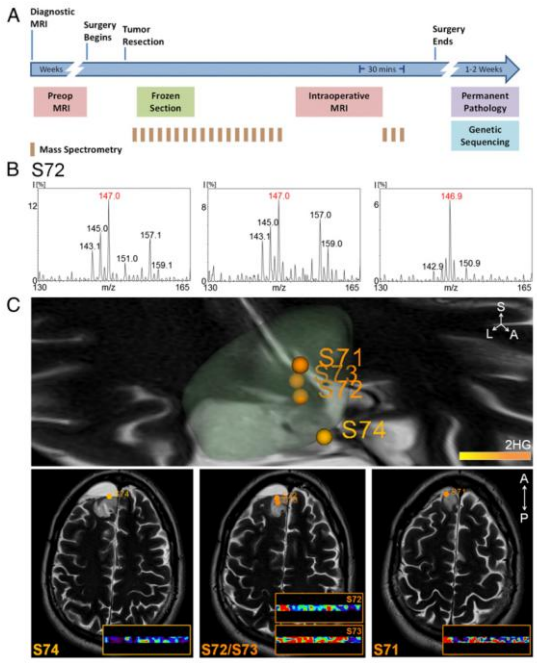

Figure 3. (A) Time course and workflow of patient care associated with a typical 5-h neurosurgery in the AMIGO, MRI-equipped, operative suite at Brigham and Women's Hospital. (B) Negative ion mode DESI mass spectra obtained using an amaZon Speed ion trap from m/z 130–165 (Bruker Daltonics) from a swab (Left), a smear (Center), and a section (Right) for sample S72. (C) Normalized 2-HG signal is represented with a warm color scale as indicated by the scale bar, set from the lowest (yellow) to highest (orange) levels detected from this individual case. Stereotactic positions were digitally

registered to the preoperative MRI using neuro navigation (BrainLab system) in a standard operating room. The 3D tumour volume is shown (Upper). Classification results of samples S74, S72, S73, and S71 are further visualized on axial sections (Lower). (Figure included with permission from Santagata et al., 2014) (Santagata et al., 2014)

Rapid evaporative ionization mass spectrometry (REIMS) is a real-time methodology that can integrate into the existing surgical workflow for the removal of brain tumours. REIMS connects an electrosurgical knife to a mass spectrometer (known as an intelligent knife or iKnife) and aerosol created during electrosurgical resection is further transferred to mass spectrometer. REIMS MS/MS can be used to measure lipid profiles and information is provided within a few seconds (Duhamel et al., 2022; Ma et al., 2021)

Further, MALDI-MSI was employed on a cohort of 46 patients to spatially resolve molecular features in glioblastoma. To validate the results, a procedure was followed by an ambient MS technique known as SpiderMass (Duhamel et al., 2022; Saudemont et al., 2018). SpiderMass technology prioritizes minimal invasiveness, enabling tissue analysis without causing extensive tissue damage. The technology relies on a micro-sampling probe which employs laser desorption of the analytes. SpiderMass operates under ambient conditions, several meters away from the mass analyzer. The system achieves this by resonantly exciting the endogenous water in biological tissues, leveraging water's abundant presence (>50%) as a MALDI matrix that solvates a broad spectrum of molecular species (Ogrinc et al., 2019; Saudemont et al., 2018).

To maximize the clinical usefulness of intraoperative real-time MS, a comprehensive reference database that catalogue the molecular profiles of healthy and diseased tissues should be readily available. Such databases serve as a foundation for interpreting the mass spectra obtained during surgery and distinguishing between normal and pathological states. Without such prior knowledge, it would be challenging to determine whether the detected proteins, lipids, or metabolites are indicative of healthy or diseased tissue.

Several initiatives are underway to characterize the molecular signatures of various tissues using MS-based technologies. For example, the Human Protein Atlas project is systematically mapping the human proteome across multiple organs using mass spectrometry and antibody-based profiling. Another

example is the Proteome Xchange (PX) consortium, an international collaboration of proteomics databases and resources aiming to standardize the dissemination of MS-based proteomics data (Deutsch et al., 2017, 2023; Uhlén et al., 2015; Vizcaíno et al., 2014). The consortium had grown to six members: PRIDE (A repository for proteomic datasets with tools for data analysis and visualization.) (Perez-Riverol et al., 2022), PeptideAtlas (Compiles peptide and protein identifications into a comprehensive proteomics resource.) (Desiere et al., 2006), MassIVE (A repository for sharing and accessing raw mass spectrometry datasets.), jPOST (repository focused on posting and sharing proteomics and other omics data.), iProX (database for high-throughput proteomics and proteogenomics data) (Ma et al., 2019)and Panorama Public (platform for sharing quantitative proteomics data and visualizations.). Such databases provide valuable insights into the molecular composition of healthy tissues and serve as a reference for comparison.

Establishing detailed reference databases of health and disease states will greatly enhance the clinical utility of intraoperative mass spectrometry(Pence & Mahadevan-Jansen, 2016; Tata et al., 2015). By rapidly matching the detected molecules to these databases, surgeons can make more informed decisions about tissue diagnosis and resection margins (Balog et al., 2013; Fatou et al., 2016; J. Zhang et al., 2017). Machine learning algorithms can also be trained on these reference data to automatically classify tissues based on their mass spectra, improving the speed and accuracy of intraoperative diagnosis (Calligaris et al., 2015; Santagata et al., 2014).

6. Mapping regions of proteins in GBM with mass spectrometry

Molecular imaging represents an important tool for characterization of the tissues, and determination of current state of disease. There are different imaging techniques used in diagnostics, such as positron emission tomography (PET), tomography, magnetic resonance spectroscopy (MRS) etc. Their application, as well as the development of tracers for use and clinical translation in glioma, are extensively discussed in a recent review (Li et al., 2020). Mass spectrometry imaging (MSI) provides the essential capabilities of microscopy and molecular analysis required to elucidate the spatio-molecular features of pathological tissue sections. A recent demonstration has highlighted the advantages of high mass resolution in MSI of intact proteins. Better mass resolution successfully

resolved the isotopic distribution of individual protein ions and provided clarity on protein oxidation states providing more confident assignments in MSI analyses (Spraggins et al., 2015)**.** The level of mass resolution achieved defines the molecular specificity of the analysis. MSI can be used to simultaneously capture the spatial distributions of numerous biomolecules directly from tissue, without the need for labelling. With MALDI a diverse range of substances, including proteins, peptides, glycans, lipids, metabolites, and drugs can be detected. Using a murine model of glioblastoma and 15 T MALDI-FTICR mass spectrometer, it was possible to distinguish between GBM-associated proteoforms, including proteins with interspersed and isobaric isotopomers (Dilillo et al., 2017). The study also reported a direct comparison between MALDI-FTICR and MALDI-TOF results. In the m/z range of 14,000–14,250, the MALDI-TOF MSI dataset exhibited a broad peak with a non-resolved shoulder while the corresponding region of the MALDI-FTICR spectrum reveals a series of isotopic distributions, highlighting distinct protein ions with higher resolution. Comparison of the MALDI-FTICR MSI data with LC-MS/MS analysis of regions of interest allowed identification of proteins such as pleiotropic actin-sequestering polypeptides, thymosin β4, thymosin β10, calcyclin (S100A6) and cytochrome c oxidase (CcO Ac/2Ox) which have been related to survival and recurrence of glioma (Dilillo et al., 2017; Hardesty et al., 2011). Investigation into non-targeted molecular classification utilizing MALDI mass spectrometry imaging (MALDI MSI) and microproteomics successfully identified distinct molecular signatures in anaplastic glioma tissues (Le Rhun et al., 2017). MALDI MSI performed on FF tissue sections involved digesting the proteins in-situ into peptides using trypsin on the tissue sections, followed by matrix deposition by micro-spraying. More than 2500 proteins were identified and classified into three subgroups: neoplasia, glioma with inflammation and neurogenesis which shows potential for more accurate classification of the glioma in the future (Le Rhun et al., 2017)

7. Detection of lipids

The recognition of lipid detection is growing in importance within "omics"-focused studies. In GBM, abnormal lipid metabolism is evident through changes in the expression of lipid-related genes, including sterol regulatory element-binding protein 1 (SREBP1) and fatty acid synthase (FAS), resulting in an altered lipid composition and the accumulation of more fatty acids in the surrounding brain tissue

(Shakya et al., 2021). It was reported that the formation of lipid droplets functions as a storage reservoir for lipids. These droplets typically form under stressful conditions, such as those induced by hypoxia and nutrient deprivation, and play a crucial role in regulating key metabolic processes related to cancer, cell death, apoptosis, and angiogenesis (Petan et al., 2018). The application of MSI for lipid profiling in GBM has proven to be a successful tool for distinguishing cellular subpopulations within GBM. Significant variations were observed in both lipid gene expression and total lipid content, with a notable enrichment of lipids in hypoxic organoid cores, peri-necrotic regions, and pseudo-palisading regions of primary patient tumours (Shakya et al., 2021; Wang et al., 2022). However, only a few studies have revealed insight into lipids or lipid-associate metabolome of brain tumours and showed changes in different lipid classes as acylglycerols, phosphatidic acids, and fatty acids (Wildburger et al., 2015a), tumoural gangliosides, sulfatides, phosphatidylinositols (He et al., 2007), and sphingolipids (Abuhusain et al., 2013). Spatially resolved ambient MS techniques such as desorption electrospray ionization MS (DESI-MSI) and picosecond infrared laser MS (PIRL-MS) imaging have recently demonstrated a gradient of lipid-associated metabolomes dependent on distance from tumour margins in medulloblastoma (Woolman et al., 2021). It was reported that brain cells in proximity to the medulloblastoma cancer border, within approximately 1.2 mm, exhibit an altered metabolic state resembling that of cancer cells. MALDI-MSI revealed the spatial clustering of lipids in distinct sections of the tumour-affected brain, providing evidence of their association with tumour pathology (Wang et al., 2022). In a study involving 39 subjects, DESI-MS was used to determine spatial distribution of different lipid classes including phosphatidylethanolamine (PE), phosphatidyl- choline (PC), phosphatidylserine (PS), sphingomyelin (SM), ceramide (Cer), phosphatidylinositol (PI), and sulfatide (ST) (Jarmusch et al., 2016). Data were recorded in both, positive and negative ionization modes, by modifying previous approach of Janfelt et al., (Janfelt et al., 2013) and using morphology preserving solvents as DMF and ACN. Data showed difference in lipid profile in white matter, grey matter and glioma; and the lipid profiles obtained in positive ion mode demonstrated a differentiation ability that was comparable to the negative ion lipid profiles. In a study to investigate the effect of TMZ on treatment, a total of 32 histological sections (four sections for each treatment and ionization mode) obtained from four distinct patients were analyzed using MALDI-IMS. MBT or DAN were used as

matrix for positive- or negative-ion detection, respectively and analyzed 124 lipid species from 11 lipid classes. Results showed altered lipid profiles in healthy brain tissue compared to tumour with a significant increase in phosphatidylethanolamine (PE), phosphatidylinositol (PI), and sphingomyelin (SM) in GBM, and a decrease in sulfatide class content (Figure 4) (Maimo-Barcelo et al., 2022).

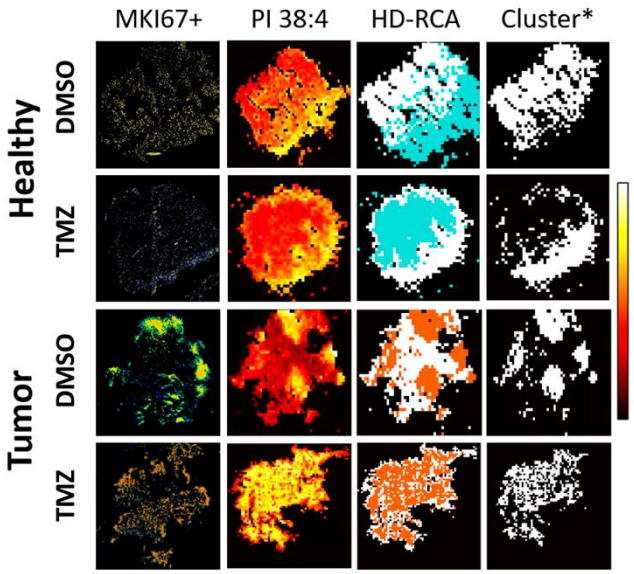

Figure 4. Brain proliferation zones and MALDI-IMS clustering comparison. Representative images of IF and MALDI-IMS for both healthy and tumour treated and non-treated are shown. Healthy brain and GBM biopsy sections were prepared after incubating fresh biopsies in DMSO (vehicle) or TMZ (10 mg/mL, 4 h) and analyzed by MALDI-IMS at 50–100 µm lateral resolution. Brain proliferation zones were determined by MKI67+ IF staining and used to select the MALDI-IMS cluster, generated by HD-RCA from consecutive tissue sections (Garate et al., 2020). HD-RCA clustering enabled the identification of the IMS regions of interest (Cluster*) with greater correlation (evaluated by direct visual inspection) with the MKI67+ IFs, based on the similarity of lipidomic content in each MALDI-IMS experiment. Proliferation zones are marked in orange in MKI67+ IFs. DAPI was used as a nucleus marker (marked in blue on IF MKI67 images). The distribution of PI 38:4 (885.55 m/z) is shown as a representative MALDI-IMS lipid distribution. Color scale indicates the intensity of the PI 38:4 -H distribution (0, black; 1, white). HD-RCA number of segments was set from 2 to 5, with prior background noise filtration using in-house MATLAB algorithms (Garate et al., 2020). (Taken with permission from Maimó-Barceló et al.) (Maimo-Barcelo et al., 2022)

Mass spectrometry has been widely used to detect cell component changes in GBM cell lines, all with the goal to investigate the toxic mechanisms induced by external stimuli (He et al., 2007; Liu et al., 2021; Shi et al., 2023). Using MALDI-MS to profile lipids on the cell membrane of U87-MG, a GBM cell line following treatment with inducers of sodium phenylbutyrate (SPB) and all-trans retinoic acid (ATRA) showed increased abundance of unsaturated glycerophosphocholines (PC) and decreased saturated PCs with treatment (Liu et al., 2021). In another study, cells were subjected to adenovirus therapy in which the vector carries either the wildtype p53 gene or no functional gene, followed by treatment with SN-38, a topoisomerase inhibitor (He et al., 2007). Analysis of polar lipids using nano-LC FT-ICR MS and quadrupole linear ion trap MS/MS yielded hundreds of unique assignments of glyco- and phospholipids with the significant structural changes for samples treated with wild-type p53 or empty vector. Effect of p53 was significant on gangliosides with the most prominent changes in ceramides.

Moreover, there have been significant metabolic changes identified in metabolism of IDH1 mutant glioma tissue when compared to IDH1 wild-type glioma (Zhou et al., 2019). Presence of IDH1 mutation resulted in presence of shorter fatty acyls as compared to IDH1 wild-type, along with decreased triglycerides and sphingolipids, however, membrane phosphatidyl lipids remained the same.

Even though analysis of tissues and cell lines represents important source of molecular information to obtain metabolic changes in GBM, it has also been suggested that cerebrospinal fluid sensitivity represents pathological changes in patients (Gahoi et al., 2018; Jadoul et al., 2016; Schuhmann et al., 2010; Shen et al., 2014). The presence of proteins in CSF may arise from secretion and leakage from tumour tissues, rendering CSF a valuable source for gaining insight into the patient's status. To better understand GBM pathobiology Gahoi et al. (Gahoi et al., 2018) studied CSF from different grades of gliomas and showed an increase in different classes of immunoglobulins in higher grades of gliomas. A comprehensive proteomics analysis of CSF was performed utilizing two complementary proteomic techniques: 2D-DIGE in conjunction with MALDI-TOF/TOF MS, and iTRAQ-based quantitative proteomics combined with Q-TOF MS. This analysis revealed numerous dysregulated CSF proteins, which were linked to lipid and lipoprotein metabolism, as well as complement and coagulation cascade (Gahoi et al., 2018). In addition, CSF of GBM patients with IDH mutations shows elevated levels of

several proteins associated with the response to oxidative stress. These findings suggest that lipidomic profiling could serve as a valuable guide for assessing the effectiveness of anticancer treatments.

8. Detection of glycans

Glycosylation represents one of the prevalent forms of posttranslational protein modifications, and its aberrant patterns represent a distinctive hallmark across various types of cancer (Pinho and Reis, 2015). Glycosylation is a crucial cellular mechanism that regulates various cellular functions, and numerous studies have demonstrated abnormal glycosylation in gliomas (Bakas et al., 2020; Heijs et al., 2016; Quesnel et al., 2023; Sharma et al., 2021; Yue et al., 2023). Despite the potential for identifying biomarkers through the analysis of native glycans, their poor ionization efficiency often necessitates derivatization prior to LC-MS analysis (He et al., 2010; Hua et al., 2011). Most derivatized forms include compounds such as 2-benzoamide, aminobenzoic acid and 2-aminopyridine (Zhou et al., 2017). Derivatization of glycans with 2-aminobenzamide followed with normal phase-LC-MALDI-TOF separation has also been used for their detection in extracellular vesicles from HEK-293 and glioma cell lines (Costa et al., 2018). Enrichment in complex N-glycans was observed across the three cell lines, with minimal presence of high mannose glycans, while the cell membranes exhibited high levels of high mannose glycans. The N-glycan profiles of mouse Tu-2449 EVs displayed significant heterogeneity, showcasing di-, tri-, and tetraquaternary structures with proximal fucosylation, along with the presence of peripheral Galα3Gal structures (Costa et al., 2018).

The glycosylation status of tumour-related species influences the behaviour of cells in neoplasm, including tumorigenesis, invasion, and metastasis (Yue et al., 2023), and abnormal glycosylation patterns are associated with varied TME conditions. Alternative strategies to target glycans represent 3D glycomaterials that can be used as a tool to evaluate glycans in GBM (Stankovic et al., 2021; Tondepu and Karumbaiah, 2022). Use of 3D glycomaterials is to develop biomimetic systems that are user-friendly, cost-effective, and compatible with downstream analysis. Ultimately, the goal is to establish a dependable GBM model suitable for conducting therapy response studies in personalized medicine. Some of them include spheroids, organoid cultures or chip deposited cultures which with composition try to mimic GBM TME. Most often glycomic changes in GBM involve increased

fucosylation and sialylation of N-glycans, especially during transition from oligodendroglioma to GBM (Furukawa et al., 2015; Pieri et al., 2023). Abnormal glycosylation was identified in FFPE tissues of a mouse brain tumour model. Utilizing MALDI-MSI for N-glycans, the authors observed that low-abundance N-glycans in tumour cells exhibited elevated levels of fucosylation, while high-abundance N-glycans in tumour cells displayed oligomannose and nonfucosylated complex glycans (Toghi Eshghi et al., 2014). In a study employing MALDI-MSI, the expression of the glycan HexNAc4-Hex5-NeuAc2 was reported to be predominantly observed in the necrotic regions of high-grade canine gliomas. To investigate the surrounding environment, various regions in adjacent tissue sections underwent microdigestion, leading to the identification of haptoglobin as the underlying glycoprotein (Malaker et al., 2022).

Studies showed that cancer stem-like cells play a pivotal role in tumour initiation and sustained proliferation. In the study of He and colleagues, lectin microarray coupled with LC-MS/MS was employed to identify cell surface glycoprotein markers in a glioblastoma-derived stem-like cell line (He et al., 2010). The cell surface glycans were first investigated by fluorescence-assisted lectin microarray, and then two galactose-specific lectins Trichosanthes kirilowii agglutinin (TKA) and Peanut agglutinin (PNA) were used to capture the glycoproteins of the two cell lines by affinity chromatography. Subsequently, the glycoproteins were identified by LC-LTQ MS and quantified by the spectral counting method. Furthermore, to delve deeper into the role of glycans in GBM progression, a recent study was conducted using glioma stem cell xenografts (Larsson et al., 2018; Wildburger et al., 2015b). The study showed differences in glycans expression between those that attracted bone marrow-derived human mesenchymal stem cells (BM-hMSCs) and those that do not. They also showed elevated occurrence of high mannose type N-glycans in the non-attractor group and further demonstrated the predominance of terminal sialic acid-containing N-glycans in non-attractors, while terminal galactose and N-acetyl-glucosamine N-glycans were prevalent in attractors (Wildburger et al., 2015b).

9. GBM immunopeptidome

Immunotherapy approaches encompass various methods, including vaccines, which can be categorized based on their sensitization target into whole tumour vaccines, tumour-associated antigens (TAAs), and

tumour-specific antigens. Cancer antigens are usually proteins or glycoproteins, that are produced by cancer cells and can trigger an immune response. TSAs are unique to cancer cells and arise from DNA mutations that lead to abnormal proteins, recognized as foreign by the immune system (Z. Zhang et al., 2021). Whilst TAAs are present in both cancer and normal cells but are overexpressed in cancer cells. These antigens, being largely cancer-specific or overexpressed in cancer, serve as markers for cancer detection, diagnosis, and treatment. Vaccines targeting TSAs or TAAs can enhance the immune system's cancer-fighting ability. Moreover, oncolytic viruses that are genetically modified to selectively infect and kill cancer cells are being used. These viruses can be engineered to express cancer antigens, further enhancing the immune system's ability to recognize and eliminate cancer cells (Lin et al., 2023). Additionally, there are cell-based therapies that involve administering sensitized and activated effector immune cells to patients, with the aim of targeting tumour cells. Another approach involves immune checkpoint modulators, which employ antibodies to block inhibitory immune checkpoint molecules like PD-1 and PDL1 (Mangano et al., 2018; Reardon et al., 2017; Srinivasan et al., 2017).

MS plays a vital role in proteome exploration and is extensively utilized in clinical settings to analyze patient samples and guide treatment decisions (Table 2). Recent advancements in MS technology have enhanced the identification and targeting of cancer-specific antigens, forming the foundation for antigen-specific therapies. The pioneering work of Hunt et al. in the 1990s introduced the sequencing of the immunopeptidome (Hunt et al., 1992). Predicting cancer-specific antigens remains a significant challenge in immunotherapy and the accurate identification of peptide neoantigens is crucial for personalized anti-tumour treatments, highlighting the indispensable role of MS in mapping the tumour immunopeptidome (Bedran et al., 2022; Kote et al., 2020)

So far, studies have focused on targeting human leukocyte antigen (HLA)-binding peptides across various cancer types, including melanoma, breast, and brain tumours, using cell lines and tissue samples (Buser et al., 2019; Giampa et al., 2016; Lombardi et al., 2015; Pusch et al., 2011; Yanovich-Arad et al., 2021). Detecting the immunopeptidome may facilitate the inclusion of tumour-associated neoantigens in vaccine formulations and enhance understanding of the pathways involved in peptide presentation on the cell surface. Loading peptides onto HLA complexes represents a pivotal stage in peptide presentation. Within the Antigen Processing and Presentation Machinery (APPM), the peptide

loading complex (PLC) is responsible for translocating peptides into the endoplasmic reticulum (ER) and ensuring the placement of appropriate peptides into the HLA binding grooves (Shapiro and Bassani-Sternberg, 2023). In one study, authors found >6000 HLA-bound peptides from HLA-A*02+ glioblastoma, whereas over 3000 were restricted by HLA-A*02 (Dutoit et al., 2012). The study aimed to investigate 10 antigens associated with GBM, and their selection was based on their elevated expression in tumours, minimal or non-existent expression in healthy tissues, involvement in gliomagenesis, and their ability to trigger an immune response.

A study investigating the immunopeptidome associated with HLA molecules in 142 plasma samples, focused on the plasma-soluble HLA molecules (sHLA) and looked at the membranal HLA in 10 samples obtained from the GBM patients (Shraibman et al., 2019). The analysis of the HLA peptidome used 52 distinct HLA allotypes and led to the identification of over 35,000 unique HLA peptides. Several hundred peptides originated from TAAs and newly characterized potential cancer-testis antigens (CTAs). Thus, these peptides could serve as valuable biomarkers and potential candidates for immunotherapeutic strategies not only for GBM but also for various other cancer types. The source protein landscape of diffuse intrinsic pontine glioma (DIPG) cell lines was investigated to better understand the category of proteins influencing the immunopeptidome. Samples from the patient-derived SU-DIPG cell lines were analyzed on Tribrid Fusion and Q Exactive Plus mass spectrometers (Pandey et al., 2023). Comparison with the previously published study (Neidert et al., 2018), found 6% (1,240) and 2% (413) peptides when compared to GBM patients and primary brain (PB), respectively. The proportion of shared proteins was considerably higher leading to 30% (2,034) and 17% (1,134) proteins shared between those identified in patient-derived cell lines and GBM patients and PB, respectively. Dutoit et al. used HLA/peptide complexes isolated from HLA-A*02+ GBM samples to evaluate the feasibility of utilizing HLA-associated tumour peptidomes as a reservoir of tumour-associated antigens for immunotherapeutic applications (Dutoit et al., 2012). Peptides were detected on LTQ Orbitrap hybrid mass spectrometer and identified nine highly immunogenic peptides for which multi-peptide therapeutic vaccine, IMA950, was developed. The IMA950 adjuvanted with Poly-ICLC (polyinosinic-polycytidylic acid stabilized with polylysine and carboxymethylcellulose) was tested for safety and immunogenicity in phase I/II study (Migliorini et al., 2019). Results showed the presence of

multi-peptide CD8 and prolonged T helper 1 CD4 T-cell responses. In the study 63.2% of the patients exhibited CD8 T-cell responses to a single peptide, while 36.8% showed responses to multiple peptides. The median overall survival for GBM patients was 19 months. Furthermore, a potential link between bacterial pathogens, the bacterial gut microbiota, and the specific immune recognition of tumour antigens has been investigated, and it was found that both glioblastoma tissues and tumour cell lines display peptides specific to bacteria within their HLA molecules (Naghavian et al., 2023).

In cancers other than GBM, Schuster et al., performed MS-based profiling of the HLA peptidome of ovarian cancer and uncovered a diverse repertoire of TAAs that can be exploited for vaccine development (H. Schuster et al., 2017). Proteomic analysis of colorectal cancer tissues has also revealed a wide range of TAAs, such as CEA and MUC1, which have been targeted by peptide-based vaccines in clinical trials (Wagner et al., 2018; Wu et al., 2022). In haematological malignancies, MS has been instrumental in identifying novel TAAs, such as the NPM1 mutation-derived peptides in acute myeloid leukemia, which have shown promise as targets for immunotherapy (Greiner et al., 2013). Furthermore, MS-based phosphoproteomics has enabled the identification of tumour-specific phosphopeptides that can serve as neoantigens for personalized cancer vaccines (Abelin et al., 2015; Zarling et al., 2006)). As MS technologies continue to advance, the integration of proteomics with genomics and immunopeptidomics will accelerate the discovery of novel cancer antigens and guide the development of more effective antigen-specific immunotherapies.

10. Clinical Applications of Proteomic Data in GBM

Over the recent years, the use of proteomics as a clinical and diagnostic tool has seen significant growth and advancement, particularly offering avenues for the identification of novel biomarkers for therapeutic purposes, potential drug targets and early diagnostics. For example, a recent study integrated the proteomics profile of blood plasma with genomic data to identify protein biomarkers and drug targets for colorectal cancer (Sun et al., 2023). Xing et al. reported MS-based proteomics by utilizing serum as liquid biopsy for early diagnosis of and even early prediction of hepatocellular carcinoma (Xing et al., 2023). In GBM context, Ye and colleagues used MS to generate proteomic profiles of U87

cell line to investigate long noncoding RNA HULC implicated in GBM progression and quantified 4360 proteins of which 112 and 24 were up- and down-regulated proteins, respectively (Ye et al., 2021). In contrast to whole-genome sequencing or transcriptome sequencing which merely suggests the source of tumours, proteomics provides insights into the current state of tumour cells by quantifying the levels of active proteins that regulate cellular functions. Another advantage of protein-based biomarkers is their increasing utility in diagnostic and prognostic across various tumours including glioblastoma. These biomarkers exhibit widespread expression in cancer tissues (Zhou et al., 2020), and can be quantified in body fluids such as blood (Lange et al., 2014), and CSF (Liu et al., 2014).

While nucleic acids are often considered highly specific due to their unique sequences, the advancements in MS technology have indeed enhanced the specificity and utility of protein analysis (Feng et al., 2021). Therefore, the combination of transcriptomics and proteomics would provide a comprehensive overview of the tumour, for example, a recent study integrated RNA-seq and proteomics data to identify a GBM surfaceome signature, which included key cell-surface genes like HLA-DRA, CD44, SLC1A5, EGFR, ITGB2, and PTPRJ1. These genes were found to be significantly upregulated in GBM and associated with poor disease-free survival (Syafruddin et al., 2021). Moreover, the Drugbank database has been used to identify clinically approved drugs targeting these GBM molecular signatures, suggesting potential for drug repurposing (Syafruddin et al., 2021). Another example was reported by Petralia et al., where a comprehensive proteo-genomic analysis for various childhood brain cancers was performed to explore novel biomarkers (Petralia et al., 2020). Additionally, generating extensive full proteomics tumour profile presents an opportunity to compare both natural and posttranslational modifications during cancer development. This approach could lead to a more specific elucidation of the mechanisms underlying tumour development, potentially resulting in the discovery of novel biomarkers and innovative treatment strategies. (Chen et al., 2021; Petushkova et al., 2017; Silantyev et al., 2019). A nicely summarized review by Kyoungho Suk about the utilization of a proteomic approach to investigate glioma drug resistance demonstrated proteins like lipocalin 2 (LCN2) and integrin β3 (ITGB3) as key proteins that determine the survival and death of glioma cells (Suk, 2012) emphasizing that proteomic profiling could explore novel aspects of cancer biology.

11. Conclusions and Future Perspectives

Mass spectrometry has a major role in detection and identification of key molecular features in GBM. Understanding the GBM tumour microenvironment is widely recognized across various research fields, all aimed at discovering effective therapies. The use of MS for protein detection stands as the foremost technique for assessing protein levels and potentially identifying biomarkers in GBM, offering high precision and reproducibility in protein quantification. It enables extraction of molecular data from GBM, including examination of protein and metabolite composition and their spatial distribution using MSI. This approach holds the potential to determine possible interactions among metabolites and gain a deeper understanding of the underlying mechanisms of oncogenesis. The incorporation of clinically relevant organotypic slice culture in proteomic studies could provide a better prediction of drug response and elucidate the underlying mechanisms of drug resistance, ultimately guiding the development of more effective treatment strategies. The assistance of histopathological annotations provided by pathologists; as well as major genetic stratifications such as CDKN2A/IFNA gene deletions provided by informatics tools, and their alignment with MS data will be an important approach in the identification of potential therapeutic targets that align with the tumour's pathological features. Key MS-derived targets can facilitate the development of new surgically guided antibody imaging tools and/or new therapeutics. Further development of some MS tools integrated into the operating room could significantly impact surgical removal of the tumour. The on-site detection and identification of tumour-related features can assist in guiding surgery to efficiently excise the tumour. Although numerous studies focus on detecting potential GBM biomarkers, there is a shortage of reports on studies utilizing integrated datasets from multiple detection sources. Studying the interaction among diverse classes of genetically stratified biomarkers, including proteins and metabolites, along with their distribution across different regions of the GBM tumour microenvironment, could provide crucial insights into tumour advancement.

AUTHOR CONTRIBUTIONS

Sofian Al Shboul: Conceptualization; Data curation; Formal analysis; Methodology; Writing - original draft; Writing - review & editing. **Ashita Singh:** Data curation; Formal analysis; Methodology; Writing

- original draft; Writing - review & editing; **Renata Kobetic:** Conceptualization; Formal analysis; Methodology; Writing - original draft; Writing - review & editing. **David R. Goodlett:** Conceptualization; Writing - original draft; Writing - review & editing. **Paul M Brennan:** Formal analysis; Methodology; Writing - original draft; Writing - review & editing. **Ted Hupp:** Conceptualization; Formal analysis; Methodology; Writing - original draft; Writing - review & editing. **Irena Dapic:** Conceptualization; Data curation; Formal analysis; Methodology; Supervision; Visualization; Writing - original draft; Writing - review & editing.

ACKNOWLEDGMENT

Sofian Al Shboul is supported by Grants No. 785/48/2022 and 738/54/2022 provided by the Deanship of Scientific Research, The Hashemite University. Irena Dapic is supported by Grant no. 01-1419/1-2024 by the Program to strengthen young scientists MZ-2023.

Conflict of Interest

The authors have no conflicts of interest to disclose.

12. References

Abelin, J. G., Trantham, P. D., Penny, S. A., Patterson, A. M., Ward, S. T., Hildebrand, W. H., Cobbold, M., Bai, D. L., Shabanowitz, J., & Hunt, D. F. (2015). Complementary IMAC enrichment methods for HLA-associated phosphopeptide identification by mass spectrometry. Nature Protocols, 10(9), 1308–1318. https://doi.org/10.1038/nprot.2015.086

Balog, J., Sasi-Szabó, L., Kinross, J., Lewis, M. R., Muirhead, L. J., Veselkov, K., Mirnezami, R., Dezso, B., Damjanovich, L., Darzi, A., Nicholson, J. K., & Takáts, Z. (2013). Intraoperative tissue identification using rapid evaporative ionization mass spectrometry. Science Translational Medicine, 5(194). https://doi.org/10.1126/scitranslmed.3005623

Berg, H. E., Halldórsson, S., Bakketeig, E. A., Thiede, B., Sandberg, C. J., Lundanes, E., Vik-Mo, E., & Wilson, S. R. (2022). Micro-pillar array columns (μPAC): An efficient tool for comparing tissue and cultured cells of glioblastoma. Journal of Chromatography Open, 2. https://doi.org/10.1016/j.jcoa.2022.100047

Calligaris, D., Feldman, D. R., Norton, I., Brastianos, P. K., Dunn, I. F., Santagata, S., & Agar, N. Y. R. (2015). Molecular typing of Meningiomas by Desorption Electrospray Ionization Mass Spectrometry Imaging for Surgical Decision-Making. International Journal of Mass Spectrometry, 377(1), 690–698. https://doi.org/10.1016/j.ijms.2014.06.024

Chandra, S., Parker, D. J., Barth, R. F., & Pannullo, S. C. (2016). Quantitative imaging of magnesium distribution at single-cell resolution in brain tumors and infiltrating tumor cells with secondary ion mass spectrometry (SIMS). Journal of Neuro-Oncology, 127(1), 33–41. https://doi.org/10.1007/S11060-015-2022-8

Chang, R. Y. K., Etheridge, N., Dodd, P. R., & Nouwens, A. S. (2014). Targeted quantitative analysis of synaptic proteins in Alzheimer's disease brain. Neurochemistry International, 75, 66–75. https://doi.org/10.1016/j.neuint.2014.05.011

Clavreul, A., Guette, C., Lasla, H., Rousseau, A., Blanchet, O., Henry, C., Boissard, A., Cherel, M., Jézéquel, P., Guillonneau, F., Menei, P., & Lemée, J. M. (2024). Proteomics of tumor and serum samples from isocitrate dehydrogenase-wildtype glioblastoma patients: is the detoxification of reactive oxygen species associated with shorter survival? Molecular Oncology. https://doi.org/10.1002/1878-0261.13668

Couturier, C. P., Ayyadhury, S., Le, P. U., Nadaf, J., Monlong, J., Riva, G., Allache, R., Baig, S., Yan, X., Bourgey, M., Lee, C., Wang, Y. C. D., Wee Yong, V., Guiot, M. C., Najafabadi, H., Misic, B., Antel, J., Bourque, G., Ragoussis, J., & Petrecca, K. (2020). Single-cell RNA-seq reveals that glioblastoma recapitulates a normal neurodevelopmental hierarchy. Nature Communications, 11(1). https://doi.org/10.1038/S41467-020-17186-5

Coy, S., Wang, S., Stopka, S. A., Lin, J. R., Yapp, C., Ritch, C. C., Salhi, L., Baker, G. J., Rashid, R., Baquer, G., Regan, M., Khadka, P., Cole, K. A., Hwang, J., Wen, P. Y., Bandopadhayay, P., Santi, M., De Raedt, T., Ligon, K. L., … Santagata, S. (2022). Single cell spatial analysis reveals the topology of immunomodulatory purinergic signaling in glioblastoma. Nature Communications, 13(1). https://doi.org/10.1038/S41467-022-32430-W

Desiere, F., Deutsch, E. W., King, N. L., Nesvizhskii, A. I., Mallick, P., Eng, J., Chen, S., Eddes, J., Loevenich, S. N., & Aebersold, R. (2006). The PeptideAtlas project. Nucleic Acids Research, 34(Database issue). https://doi.org/10.1093/nar/gkj040

Deutsch, E. W., Bandeira, N., Perez-Riverol, Y., Sharma, V., Carver, J. J., Mendoza, L., Kundu, D. J., Wang, S., Bandla, C., Kamatchinathan, S., Hewapathirana, S., Pullman, B. S., Wertz, J., Sun, Z., Kawano, S., Okuda, S., Watanabe, Y., Maclean, B., Maccoss, M. J., … Vizcaíno, J. A. (2023). The ProteomeXchange consortium at 10 years: 2023 update. Nucleic Acids Research, 51(D1), D1539–D1548. https://doi.org/10.1093/nar/gkac1040

Deutsch, E. W., Csordas, A., Sun, Z., Jarnuczak, A., Perez-Riverol, Y., Ternent, T., Campbell, D. S., Bernal-Llinares, M., Okuda, S., Kawano, S., Moritz, R. L., Carver, J. J., Wang, M., Ishihama, Y., Bandeira, N., Hermjakob, H., & Vizcaíno, J. A. (2017). The ProteomeXchange consortium in 2017: Supporting the cultural change in proteomics public data deposition. Nucleic Acids Research, 45(D1), D1100–D1106. https://doi.org/10.1093/nar/gkw936

Fan, Q., Wang, H., Gu, T., Liu, H., Deng, P., Li, B., Yang, H., Mao, Y., & Shao, Z. (2024). Modeling the precise interaction of glioblastoma with human brain region-specific organoids. IScience, 27(3), 109111. https://doi.org/10.1016/j.isci.2024.109111

Fatou, B., Saudemont, P., Leblanc, E., Vinatier, D., Mesdag, V., Wisztorski, M., Focsa, C., Salzet, M., Ziskind, M., & Fournier, I. (2016). In vivo Real-Time Mass Spectrometry for Guided Surgery Application. Scientific Reports, 6. https://doi.org/10.1038/srep25919

Greiner, J., Schneider, V., Schmitt, M., Götz, M., Döhner, K., Wiesneth, M., Döhner, H., & Hofmann, S. (2013). Immune responses against the mutated region of cytoplasmatic NPM1 might contribute to the favorable clinical outcome of AML patients with NPM1 mutations (NPM1mut). Blood, 122(6), 1087–1088. https://doi.org/10.1182/BLOOD-2013-04-496844

Hu, R., Li, Y., Yang, Y., & Liu, M. (2023). Mass spectrometry-based strategies for single-cell metabolomics. Mass Spectrometry Reviews, 42(1), 67–94. https://doi.org/10.1002/MAS.21704

Huang, L., Wickramasekara, S. I., Akinyeke, T., Stewart, B. S., Jiang, Y., Raber, J., & Maier, C. S. (2016). Ion mobility-enhanced MSE-based Label-free Analysis Reveals Effects of Low-dose Radiation Post Contextual Fear Conditioning Training on the Mouse Hippocampal Proteome. Journal of Proteomics, 140, 24. https://doi.org/10.1016/J.JPROT.2016.03.032

Kelstrup, C. D., Bekker-Jensen, D. B., Arrey, T. N., Hogrebe, A., Harder, A., & Olsen, J. V. (2018). Performance Evaluation of the Q Exactive HF-X for Shotgun Proteomics. Journal of Proteome Research, 17(1), 727–738. https://doi.org/10.1021/ACS.JPROTEOME.7B00602

Koopmans, F., Ho, J. T. C., Smit, A. B., & Li, K. W. (2018). Comparative Analyses of Data Independent Acquisition Mass Spectrometric Approaches: DIA, WiSIM-DIA, and Untargeted DIA. Proteomics, 18(1). https://doi.org/10.1002/pmic.201700304

Lagache, L., Le Rhun, E., Fournier, I., & Salzet, M. (2024). Prediction of protein pathways by correlation of spatial lipidomic and proteomics : towards the concept of dry proteomics applied to human Glioblastoma for patient prognosis. https://doi.org/10.21203/RS.3.PEX-2624/V1

Lee, J. K., Wang, J., Sa, J. K., Ladewig, E., Lee, H. O., Lee, I. H., Kang, H. J., Rosenbloom, D. S., Camara, P. G., Liu, Z., Van Nieuwenhuizen, P., Jung, S. W., Choi, S. W., Kim, J., Chen, A., Kim, K. T., Shin, S., Seo, Y. J., Oh, J. M., … Nam, D. H. (2017). Spatiotemporal genomic architecture informs precision oncology in glioblastoma. Nature Genetics, 49(4), 594–599. https://doi.org/10.1038/NG.3806

Lin, D., Shen, Y., & Liang, T. (2023). Oncolytic virotherapy: basic principles, recent advances and future directions. Signal Transduction and Targeted Therapy, 8(1). https://doi.org/10.1038/s41392-023-01407-6

Ludwig, C., Gillet, L., Rosenberger, G., Amon, S., Collins, B. C., & Aebersold, R. (2018). Data-independent acquisition-based SWATH-MS for quantitative proteomics: a tutorial. Molecular Systems Biology, 14(8), e8126. https://doi.org/10.15252/msb.20178126

Ma, J., Chen, T., Wu, S., Yang, C., Bai, M., Shu, K., Li, K., Zhang, G., Jin, Z., He, F., Hermjakob, H., & Zhu, Y. (2019). Iprox: An integrated proteome resource. Nucleic Acids Research, 47(D1), D1211–D1217. https://doi.org/10.1093/nar/gky869

Meier, F., Geyer, P. E., Virreira Winter, S., Cox, J., & Mann, M. (2018). BoxCar acquisition method enables single-shot proteomics at a depth of 10,000 proteins in 100 minutes. Nature Methods 2018 15:6, 15(6), 440–448. https://doi.org/10.1038/s41592-018-0003-5

Muntel, J., Gandhi, T., Verbeke, L., Bernhardt, O. M., Treiber, T., Bruderer, R., & Reiter, L. (2019). Surpassing 10 000 identified and quantified proteins in a single run by optimizing current LC-MS instrumentation and data analysis strategy. Molecular Omics, 15(5), 348–360. https://doi.org/10.1039/C9MO00082H

Patel, A. P., Tirosh, I., Trombetta, J. J., Shalek, A. K., Gillespie, S. M., Wakimoto, H., Cahill, D. P., Nahed, B. V., Curry, W. T., Martuza, R. L., Louis, D. N., Rozenblatt-Rosen, O., Suvà, M. L., Regev, A., & Bernstein, B. E. (2014). Single-cell RNA-seq highlights intratumoral heterogeneity in primary glioblastoma. Science, 344(6190), 1396–1401. https://doi.org/10.1126/SCIENCE.1254257

Pence, I., & Mahadevan-Jansen, A. (2016). Clinical instrumentation and applications of Raman spectroscopy. Chemical Society Reviews, 45(7), 1958–1979. https://doi.org/10.1039/c5cs00581g

Perez-Riverol, Y., Bai, J., Bandla, C., García-Seisdedos, D., Hewapathirana, S., Kamatchinathan, S., Kundu, D. J., Prakash, A., Frericks-Zipper, A., Eisenacher, M.,

Walzer, M., Wang, S., Brazma, A., & Vizcaíno, J. A. (2022). The PRIDE database resources in 2022: A hub for mass spectrometry-based proteomics evidences. Nucleic Acids Research, 50(D1), D543–D552. https://doi.org/10.1093/nar/gkab1038

Rybin, M. J., Ivan, M. E., Ayad, N. G., & Zeier, Z. (2021). Organoid Models of Glioblastoma and Their Role in Drug Discovery. Frontiers in Cellular Neuroscience, 15. https://doi.org/10.3389/FNCEL.2021.605255

Santagata, S., Eberlin, L. S., Norton, I., Calligaris, D., Feldman, D. R., Ide, J. L., Liu, X., Wiley, J. S., Vestal, M. L., Ramkissoon, S. H., Orringer, D. A., Gill, K. K., Dunn, I. F., Dias-Santagata, D., Ligon, K. L., Jolesz, F. A., Golby, A. J., Cooks, R. G., & Agar, N. Y. R. (2014). Intraoperative mass spectrometry mapping of an onco-metabolite to guide brain tumor surgery. Proceedings of the National Academy of Sciences of the United States of America, 111(30), 11121–11126. https://doi.org/10.1073/pnas.1404724111

Schuster, H., Peper, J. K., Bösmüller, H. C., Röhle, K., Backert, L., Bilich, T., Ney, B., Löffler, M. W., Kowalewski, D. J., Trautwein, N., Rabsteyn, A., Engler, T., Braun, S., Haen, S. P., Walz, J. S., Schmid-Horch, B., Brucker, S. Y., Wallwiener, D., Kohlbacher, O., … Wagner, P. (2017). The immunopeptidomic landscape of ovarian carcinomas. Proceedings of the National Academy of Sciences of the United States of America, 114(46), E9942–E9951. https://doi.org/10.1073/PNAS.1707658114

Schuster, M., Braun, F. K., Chiang, D. M. L., Ludwig, C., Meng, C., Grätz, C., Kirchner, B., Proescholdt, M., Hau, P., Steinlein, O. K., Pfaffl, M. W., Riemenschneider, M. J., & Reithmair, M. (2024). Extracellular vesicles secreted by 3D tumor organoids are enriched for immune regulatory signaling biomolecules compared to conventional 2D glioblastoma cell systems. Frontiers in Immunology, 15. https://doi.org/10.3389/FIMMU.2024.1388769

Shen, L., Zhang, Z., Wu, P., Yang, J., Cai, Y., Chen, K., Chai, S., Zhao, J., Chen, H., Dai, X., Yang, B., Wei, W., Dong, L., Chen, J., Jiang, P., Cao, C., Ma, C., Xu, C., Zou, Y., … Chen, S. (2024). Mechanistic insight into glioma through spatially multidimensional proteomics. Science Advances, 10(7). https://doi.org/10.1126/SCIADV.ADK1721

Tata, A., Zheng, J., Ginsberg, H. J., Jaffray, D. A., Ifa, D. R., & Zarrine-Afsar, A. (2015). Contrast Agent Mass Spectrometry Imaging Reveals Tumor Heterogeneity. Analytical Chemistry, 87(15), 7683–7689. https://doi.org/10.1021/acs.analchem.5b01992

Tsou, C. C., Avtonomov, D., Larsen, B., Tucholska, M., Choi, H., Gingras, A. C., & Nesvizhskii, A. I. (2015). DIA-Umpire: comprehensive computational framework for data-independent acquisition proteomics. Nature Methods 2015 12:3, 12(3), 258–264. https://doi.org/10.1038/nmeth.3255

Uhlén, M., Fagerberg, L., Hallström, B. M., Lindskog, C., Oksvold, P., Mardinoglu, A., Sivertsson, Å., Kampf, C., Sjöstedt, E., Asplund, A., Olsson, I. M., Edlund, K., Lundberg, E., Navani, S., Szigyarto, C. A. K., Odeberg, J., Djureinovic, D., Takanen, J. O., Hober, S., … Pontén, F. (2015). Tissue-based map of the human proteome. Science, 347(6220). https://doi.org/10.1126/science.1260419

Vanbellingen, Q. P., Castellanos, A., Rodriguez-Silva, M., Paudel, I., Chambers, J. W., & Fernandez-Lima, F. A. (2016). Analysis of Chemotherapeutic Drug Delivery at the Single Cell Level Using 3D-MSI-TOF-SIMS. Journal of the American Society for Mass Spectrometry, 27(12), 2033–2040. https://doi.org/10.1007/S13361-016-1485-Y

Vizcaíno, J. A., Deutsch, E. W., Wang, R., Csordas, A., Reisinger, F., Ríos, D., Dianes, J. A., Sun, Z., Farrah, T., Bandeira, N., Binz, P. A., Xenarios, I., Eisenacher, M., Mayer, G., Gatto, L., Campos, A., Chalkley, R. J., Kraus, H. J., Albar, J. P., … Hermjakob, H. (2014). ProteomeXchange provides globally coordinated proteomics data submission and dissemination. Nature Biotechnology, 32(3), 223–226. https://doi.org/10.1038/nbt.2839

Wagner, S., Mullins, C. S., & Linnebacher, M. (2018). Colorectal cancer vaccines: Tumor-associated antigens vs neoantigens. World Journal of Gastroenterology, 24(48), 5418–5432. https://doi.org/10.3748/WJG.V24.I48.5418

Wang, C., Sun, M., Shao, C., Schlicker, L., Zhuo, Y., Harim, Y., Peng, T., Tian, W., Stöffler, N., Schneider, M., Helm, D., Chu, Y., Fu, B., Jin, X., Mallm, J.-P., Mall, M., Wu, Y., Schulze, A., & Liu, H.-K. (2024). A multidimensional atlas of human glioblastoma-like organoids reveals highly coordinated molecular networks and effective drugs. NPJ Precision Oncology, 8(1), 19. https://doi.org/10.1038/s41698-024-00500-5

Wu, Z., Yang, M., & Cao, Y. (2022). Tumor antigens and vaccines in colorectal cancer. Medicine in Drug Discovery, 16. https://doi.org/10.1016/j.medidd.2022.100144

Xu, T., Feng, D., Li, H., Hu, X., Wang, T., Hu, C., Shi, X., & Xu, G. (2022). Recent advances and typical applications in mass spectrometry-based technologies for single-cell metabolite analysis. TrAC - Trends in Analytical Chemistry, 157. https://doi.org/10.1016/j.trac.2022.116763

Xu, Y. W., Lin, P., Zheng, S. F., Huang, W., Lin, Z. Y., Shang-Guan, H. C., Lin, Y. X., Yao, P. Sen, & Kang, D. Z. (2021). Acetylation Profiles in the Metabolic Process of Glioma-Associated Seizures. Frontiers in Neurology, 12. https://doi.org/10.3389/FNEUR.2021.713293/XML/NLM

Yin, L., Zhang, Z., Liu, Y., Gao, Y., & Gu, J. (2019). Recent advances in single-cell analysis by mass spectrometry. Analyst, 144(3), 824–845. https://doi.org/10.1039/C8AN01190G

Zarling, A. L., Polefrone, J. M., Evans, A. M., Mikesh, L. M., Shabanowitz, J., Lewis, S. T., Engelhard, V. H., & Hunt, D. F. (2006). Identification of class I MHC-associated phosphopeptides as targets for cancer immunotherapy. Proceedings of the National Academy of Sciences of the United States of America, 103(40), 14889–14894. https://doi.org/10.1073/pnas.0604045103

Zhang, C., Jin, M., Zhao, J., Chen, J., & Jin, W. (2020). Organoid models of glioblastoma: advances, applications and challenges. American Journal of Cancer Research, 10(8), 2242. /pmc/articles/PMC7471358/

Zhang, F., Ge, W., Ruan, G., Cai, X., & Guo, T. (2020). Data-Independent Acquisition Mass Spectrometry-Based Proteomics and Software Tools: A Glimpse in 2020. PROTEOMICS, 20(17–18). https://doi.org/10.1002/pmic.201900276

Zhang, J., Rector, J., Lin, J. Q., Young, J. H., Sans, M., Katta, N., Giese, N., Yu, W., Nagi, C., Suliburk, J., Liu, J., Bensussan, A., Dehoog, R. J., Garza, K. Y., Ludolph, B., Sorace, A. G., Syed, A., Zahedivash, A., Milner, T. E., & Eberlin, L. S. (2017). Nondestructive tissue analysis for ex vivo and in vivo cancer diagnosis using a handheld mass spectrometry system. Science Translational Medicine, 9(406). https://doi.org/10.1126/scitranslmed.aan3968

Zhang, X. C., Zang, Q., Zhao, H., Ma, X., Pan, X., Feng, J., Zhang, S., Zhang, R., Abliz, Z., & Zhang, X. (2018). Combination of Droplet Extraction and Pico-ESI-MS Allows the Identification of Metabolites from Single Cancer Cells. Analytical Chemistry, 90(16), 9897–9903. https://doi.org/10.1021/ACS.ANALCHEM.8B02098

Zhang, Z., Lu, M., Qin, Y., Gao, W., Tao, L., Su, W., & Zhong, J. (2021). Neoantigen: A New Breakthrough in Tumor Immunotherapy. Frontiers in Immunology, 12. https://doi.org/10.3389/fimmu.2021.672356

Table 1. Summary of the mass spectrometry analysis of metabolites and proteins in human GBM samples

Biological material		Analyte	Instrumentation	Comment	Author
10 patients	Tissue biopsies (5-50 mm3) taken with 73 smears	Analysis of 2-hydroxyglutarate (2HG) in tissue sections; No 2HG was detected for IDH-wildtype tumours; 2HG was detected in the tumour core biopsies which were determined postoperatively to be IDH-mutant; intensity of 2HG was correlated with the degree of tumour infiltration	DESI-MS Linear ion trap	Intraoperative DESI-MS used for detection of tumour presence, degree and subtype, and tumour mutations; detection of 2HG (m/z 147)	Pirro et al., 2017
54 patients	4 and 10 μm thick tissue slices; 26 tumour tissues with IDH1 or IDH2 mutations, 26 IDH-wildtype tumour tissues served as controls	Detection of 2HG with MALDI-TOF showed positive correlation with biochemical assay; Tissue samples with IDH mutation showed higher signal as compared to controls	MALDI-TOF Rapiflex MALDI-TOF	Evaluation of non-commercially available matrix maleic anhydride proton sponge (MAPS)	Longuespée et al., 2019
84 patients	Three independent cohorts with total of 176 cerebrospinal fluid samples with matching tumour brain tissue	Detection and quantification of D- and L-forms of 2HG after derivatization with diacetyl-L-tartaric anhydride (DATAN); levels of D-2HG were elevated with samples with IDH 1/2 mutations	LC-MS QTRAP 5500	CSF was sampled from the ventricular system (N = 113), the cavernous or subarachnoid space of the convexities (cisternal; N = 44) or from the spinal canal (lumbar; N = 15) and four samples were of unknown origin; levels of 2HG seem to be sampling site dependent with highest values in central (cisternal or ventricular), and the lowest in distal (lumbar) CSF	Kalinina et al., 2019

8 patients' tissue, 5 epileptic patients as control	25 to 258 mg biopsy; patient-derived cell culture		LC-MS Orbitrap Lumos Tribrid	Downregulation of both clathrin-dependent and -independent endocytosis machinery; potentially implicated in tumour suppression	Buser et al., 2019
130 tissue samples, 125 blood samples, 18 control brain tissue obtained after surgery from epilepsy patients, 42 control blood samples	GBM and serum were depleted using HU-14 MARS column and labelled using 4-plex iTRAQ reagents	high abundance of serum S100A8/S100A9; positive correlation between S100A8 and S100A9 transcripts and serum proteins	LC-MS Thermo LTQ	High expression levels of S100A8 and S100A9 suggest their potential as markers associated with survival prediction	Arora et al., 2019
15 FF tissues, 15 FFPE, patient-derived culture (2 IDHwt and 1 IDHmt)	10 µm FFPE, bulk FF and cell culture		LC-MS Q Exactive Plus	Approx. 2500 proteins identified from FFPE tissues and nearly 2500 from FF tissues; tumours with no IDH mutation had higher levels of proteins associated with invasiveness and epithelial to mesenchymal transition, whereas IDH-mutant gliomas showed elevated levels of proteins involved in mRNA splicing	Djuric, et al. 2019
5 FFPE tissues	4 µm, 10 µm, and 15 µm thick FFPE tissue sections		LC-MS Orbitrap Exploris	DIA-MS of GBM FFPE tissue sections; detection of immune related proteins and VIM overexpression linked to poor survival in GBM patients	Weke et al., 2022

Isolated CD4+ T cells; 15 µm and 20 µm FFPE tissues	15 um and 20 um FFPE tissues with approx. 16 mm^2 area		LC-MS 1. LTQ XL Orbitrap 2. TripleTOF 5600+	Evaluation of LC-MS methods of FFPE GBM tissue and CD4+ cells on two LC-MS platforms; Filter-aided sample preparation (FASP), traditional in-solution digestion (ISD), and a pressure-assisted (PCT) methods were used to analysed isolated CD4+ T cells and GBM FFPE tissue samples	Pirog et al, 2021
22 glioma patients, 25 benign brain tumour patients, 28 no-brain tumour patients	CSF		SELDI-TOF PBS-II SELDI-TOF-MS platform	Study used fingerprint diagnostic models of CSF proteins to differentiate protein signatures in patients with glioma and benign brain tumour; Seven potential biomarkers were identified to distinguish glioma from non-brain tumour; eight potential biomarkers were identified to distinguish glioma from benign brain tumour	Liu et al., 2014
10 GBM and 10 epilepsy FF tissue specimen			LC-MS LTQ-Orbitrap Velos	Gel based sample fractionation followed by LC-MS; known GBM-associated proteins and novel potential biomarkers were identified including CLIC4, NP1L1, IGKC, TAGL2, and YES involved in cancer progression	Heroux et al., 2014

99 GBM tissue and blood samples collected from 10 tissue source sites; 10 normal samples from the frontal cortex	Approx. 50 mg snap-frozen tissue 11-plex TMT		LC-MS Orbitrap Fusion Lumos	Integrated analysis of genomic, proteomic, post-translational modification and metabolomic data; positive correlation between H2B acetylation and patterns of protein expression associated with immune cell functions in GBM	Wang et al., 2021
14 GBM tissue and plasma specimen; 15 plasma samples from healthy subjects	GBM tissue Plasma; Cyst fluid; Two noncancerous brain tissues		LC-MS Triple TOF 5600	SWATH-MS analysis of GBM samples; High expression of LRG1, C9 and alpha-1-antichymotrypsin (SERPINA3) in the GBM plasma as compared to control plasma; Low expression of GSN, IGHA1, and apolipoprotein A-IV (APOA4) in the GBM plasma as compared to control plasma	Miyauchi et al., 2018
24 patient; 50 healthy control	Plasma	seven biomarkers were higher in GBM relative to control: Pyruvate, 5-Hydroxymethyluracil, Arginyl-Proline, Phosphatidylserine, 3-O-Sulfogalactosylceramide, 3-Oxodecanoyl-CoA and NAPE (N-acylphosphatidylethanolamine)	ESI-LTQ	Arginyl-proline was the most frequent metabolite;	Ferrasi et al., 2023

65 GBM; 17 G-2 (astrocytoma)	Plasma; GBM U87 cell culture medium TMT	Exploring plasma extracellular vesicle (plEV) for novel prognostic and diagnostic markers	LC-MS High-resolution isoelectric focusing (HiRIEF)	* 772 proteins were overlapped between GBM patients' plasma and gcEVs. * Syndecan-1 (SDC1) as a plasma extracellular vesicle (plEV) constituent for noninvasive differentiation between GBM and LGG and plEVSDC1 correlated with SDC1 in GBM tumour tissue	Chandran et al., 2019
29 primary GBMs	Tissue; Plasma	Targeted and untargeted Metabolic phenotyping	LC-MS MALDI LC-Synapt G2 FTICR-SolariX XR	176 differentially expressed lipids and metabolites, 148 in plasma and 28 in tissue samples; Main classes include phospholipids, acylcarnitines, sphingomyelins, and triacylglycerols	Gilard et al., 2021
43 recurrent GBM patients; 43 age- and sex-matched healthy controls	Tissue Blood TMT	Tryptophane and its direct downstream metabolite FK, were less abundant in necrotic or hypervascularized regions	LC-MS MALDI MSI Triple Quadrupole TSQ Vantage FTICR-SolariX	Levels of tryptophan and its metabolites were decreased in the serum of patients with GBM which was negatively correlated with tumour volume	Panitz et al., 2019
54 tumour samples: 17 LGG without malignant transformation, 18 patients LGG and their consecutive	Tumour tissue	Ratios of 2-HG/isocitrate were used to evaluate differences in 2-HG accumulation in tumours from LGG and sGBM groups, compared with pGBM and non-glioma groups.	LC-MS QTRAP 5500 triple quadruple	2HG accumulation is not suitable as an early biomarker for distinguishing patients with LGG in relation to their course of malignancy	Juratli et al., 2013

secondary glioblastomas (sGBM; n = 36) 2 sGBM 10 primary glioblastomas (pGBM) 7 patients without gliomas.					
33 GBM patients treated with bevacizumab and evofosfamide	Blood	Blood circulating metabolites biomarkers of tumour hypoxia; Untargeted approaches and characterized changes in circulating metabolite levels during treatment with combined bevacizumab and evofosfamide in recurrent GBM after bevacizumab failure	LC-MS Q Exactive Hybrid Quadrupole Orbitrap mass spectrometer	Gamma aminobutyric acid, glutamic acid and D-glutamic acid all inversely correlated with tumor hypoxia; Lactic acid was modulated by treatment, likely in response to a hypoxia mediated modulation of oxidative vs glycolytic metabolism	Lodi et al., 2022
87 patients (54 MS, 65 RNA-seq, and 32 had both)	Tumour FFPE sample; TMT	Identified 7,096 proteins which split samples into three groups	LC-MS Q-Exactive HF	Confirmed connection between stemness, metabolism, and overall survival in GBM	Yanovich-Arad et al., 2021

42 patients paired samples; newly diagnosed and recurrent GBM	FFPE SWATH-MS		LC-MS TripleTOF 6600	BCAS1, INF2, and FBXO2 were consistently upregulated proteins at recurrence and validated these using IHC	Buehler et al., 2023
Human normal cortex (N = 29); Lower-grade astrocytoma (N = 19); GBM (N = 28).	FF	Analyse CL structural diversity in astrocytomas of varying grades and correlate with histological regions within the heterogeneous astrocytoma microenvironment	DESI-FAIMS-MS DESI 2DTM system coupled to a Q Exactive	GBM cardiolipin profiling correlated with trends in tumour viability and infiltration; Structural characterization revealed differences in fatty acid and double bond isomer composition among astrocytoma tissues compared with normal cortex and glioblastoma tissues	Krieger et al., 2023
20 GBM IDH-wildtype	FFPE; 86 laser capture microscopy (LCM) samples; region-agnostic approach to define heterogeneity in GBM tumor regions.	Total of 4794 proteins were detected;	LC-MS Q Exactive HF-X	Two distinct proteogenomic programs were defined (MYC- and KRAS-axis hereon) that cooperate with hypoxia to produce a tri-dimensional model of intra-tumoral heterogeneity which was used to assess drug sensitivities and relative chemoresistance in glioblastoma cell lines with enhanced KRAS programs	Brian Lam et al., 2022

14 GBMs; 4 controls	Blood	Accumulation of ceramides, total polar lipids (TPLs), diacylglycerol (DAGs), TAGs, and sphingomyelins (SMs) in GBM	LC-MS Q-TOF	Investigation of the potential of blood lipids for use as biomarkers for the diagnosis of GBM via untargeted lipidomic approach	Soylemez et al., 2023
73 primary GBM (12 used for MALDI-IMS)	FFPE	Protein distributions in microvascular niche patterns (MVNPs)	MALDI-IMS UltrafleXtreme MALDI-TOF/TOF	GBMs were classified into two MVNPs. MALDI-MS successfully discriminate between the different types of molecules in tissue specimens that are associated with vascular distribution	Chen et al., 2022
25 primary GBM IDH-wt; 6 low-grade IDH-mut	FF	Metabolic alterations between tumour and peritumoural tissue in human GBMs; Increased levels of the antioxidants ascorbic acid, taurine, and glutathione in tumour; Increased levels of purine and pyrimidine metabolism compounds in tumour; Increased lactate and glutamine, and decrased N-acetylaspartate in GBM	MALDI-TOF MALDI-RapifleX	Antioxidants are enhanced in GBM Fatty acids were found to be decreased in GBM areas compared to peritumoral tissue areas	Kampa et al., 2020

45 glioma patients: G-II n=8 G-III n=16 GBM n=21 12 normal brains U87 cell line Xenograft	FFPE and FF	Intratumoural heterogeneity was investigated with high spatial resolution	MSI TOF-SIMS	Staining with gold-conjugated antibodies against Caveolin-1 visualized boundary between necrotic and cellular tumour zones, and enabled grouping according to survival	Gularyan et al., 2020
36 GBM IDH-WT	105 plasma samples: before surgery (n=36) , two days after surgery (n=32), prior to starting radiation therapy (n=28), and after completing radiation therapy (n=17).	Untargeted plasma metabolomics; After radiation decreased levels of glycine, serine, threonine, oxoproline, 6-deoxyglucose, gluconic acid, glycerol-alpha-phosphate, ethanolamine, propyleneglycol, triethanolamine, xylitol, succinic acid, arachidonic acid, linoleic acid, and fumaric acid; After chemoradiation decreased levels of 3-aminopiperidine 2,6-dione	GC-TOF MS Agilent 6890 GC	157 unique metabolites were identified; Characterization of metabolite patterns changes in GBM patients undergoing surgery and concurrent chemoradiation using machine learning algorithms;	Aboud et al., 2023

27 patients: 27 core and infiltrating edge samples from same patient (54 samples)	FF	Identification of clinically relevant metabolomics to act as predictors of survival from tumour core versus edge tissues Distinct relative abundances were found for DL-alanine, creatine, cystathionine, nicotinamide, and D-pantothenic acid;	2D-LC-MS Q Exactive HF	66 metabolites were found to significantly differ between glioma core and edge regions; Quantitative enrichment analysis revealed significant metabolic pathways such as glycerophospholipid metabolism, butanoate metabolism, cysteine and methionine metabolism, as well as glycine, serine, alanine, and threonine metabolism. Additionally, purine metabolism, nicotinate and nicotinamide metabolism, and pantothenate and coenzyme A biosynthesis were identified as significant pathways.	Baxter et al., 2023
21 sample: 6 GBM 6 G-III 6 G-II 3 controls (epilepsy)	FF iTRAQ	5,623 peptides were identified which mapped to 743 proteins. Of these, a total of 244 proteins were differentially expressed. Further analysis revealed YBX1 as a potential regulator of key molecules involved in tumour invasion.	LC-MS LTQ - Orbitrap Velos	Investigation of differentially regulated nuclear proteome of GBM and lower grades of gliomas (Grade II and III)	Gupta et al., 2019

36 patients: 11 GBM 3 anaplastic astrocytomas, G-III 3 diffuse astrocytomas, G-II 6 oligodendroglioma, G-II 2 anaplastic oligodendrogliomas, G-III 11 control samples	Intra-operative; 124 mass spectra biopsy were taken from 36 patients	To develop and validate MS technique for the molecular characterization of high- and low-grade glioma tissue during surgery; Mostly identified phosphatidylethanolamines (PE) followed by phosphatidic acids (PA), sphingolipids (SP) and fatty acids (FA)	REIMS and iKnife MALDI REIMS-Xevo G2-XS QTOF Orbitrap Elite	Statistical model could differentiate between normal brain, G II-III (oligodendroglioma or astrocytoma and GBM with an 88% overall accuracy.	Van Hese et al., 2022
43 GBM 25 different central nervous system malignancies 33 healthy controls	Plasma	Plasma EVs concentration was higher in GBM compared with controls brain metastases and extra-axial brain tumors ($P < 0.001$);	LC-MS Orbitrap Q Exactive-HF	Investigation of potential role of plasma extracellular vesicles (EVs) from patients with GBM for diagnosis and follow-up after treatment and as a prognostic tool; Level of EVs in recurrent GBMs was higher relative to matched primary GBM	Osti et al., 2019
15 GBM and 10 healthy control	Blood Plasma	Total of 141 proteins were identified between GBM and control of which 94 proteins significantly differentially expressed (93 enriched in GBM.	LC-MS Q Exactive	Proteomic characterization of small EVs to identify potential candidate GBM biomarkers; Inflammatory biomarker signature comprising members of the complement and regulators of inflammation and coagulation	Cilibrasi et al., 2022

37 GBM samples; 51 biopsies from 25 patients (14 IDH-wt and 11 IDH-mut)	FF tumour tissues; Intraoperative MS	Differences were detected in 2HG between IDH-WT and IDH-mut samples; Detection of glutamate, aspartate, N-acetylaspartate, and phosphocholine	DESI-MS LTQ	Detection of oncometabolite in IDH-mutant gliomas, 2HG; Subsequently, this approach was used intraoperatively to analyze tissue smears obtained from glioma patients undergoing resection and to rapidly diagnose IDH mutation status (< 5 minutes)..	Alfaro et al., 2020
18 GBM samples and 15 controls	Blood Plasma	Leucine and phenylalanine decreased in GBM with lost ATRX expression on IHC Majority of AA were lowered in GBM	LC-MS TripleTOF 4600	Investigation of the role of amino acids on regulating the metabolic pathways necessary for maintenance and growth of GBM	Bobeff et al., 2021
20 gliomas: 10 EGFR-positive and 10 EGFR-negative	FF iTRAQ	4531 proteins per EGFR-positive; 4324 proteins per EGFR-negative ; 322 proteins were significantly different of which 181 proteins were up-regulated and 141 proteins were down-regulated in EGFR-positive tumours compared with those in EGFR-negative	LC-MS Orbitrap Q Exactive HF	Screening EGFR-related proteins to identify proteins that are differentially expressed among different subsets of patients with gliomas.	Wang et al., 2020
26 GBM (24 IDH-wt and 2 IDH-mut); 9 G-III (IDH-mut),	Plasma (EVs)	4909 EV-associated proteins were identified of these, 11 proteins were exclusively found in plasma-EVs from	SWATH-MS TripleTOF 6600	Comprehensive proteomic profiling of circulating-EVs	Hallal et al., 2020

6 G-II (IDH-mut); 5 non-glioma control; 6 healthy controls		GBM patients (AIDA, ARHGEF10, BNIP3L, FYB1, KMT2D, MAP7, MAST4, PDE8A, POLR2D, RENBP and SLC25A17)			
10 patients: 7 recurrent GBMs and 3 brain metastases	Tumour Plasma CSF	Patients with high expression of pSTAT5b/pFAK/pIGFR1 were administered ceritinib for 10 days prior to tumour resection	LC-MS QTRAP 6500 (method from Bao et al., 2018)	Phase 0 trial measured the tumour pharmacokinetics and pharmacodynamics of ceritinib; High binding of ceritinib to plasma proteins and brain tumour tissues	Mehta et al., 2022
30 GBM; 24 Meningioma	Blood	Comparison of GBM with the control group, showed differences for lysine, histidine, α-aminoadipic acid, and phenylalanine; Comparison of meningioma patients with the control group, showe differences only for lysine	LC-MS LCMS-8045	Evaluation of potential of targeted dual-control serum amino acid metabolomics analysis in the diagnosis of patients with glioma and meningioma	Kośliński et al., 2023
13 GBM; 6 controls	FF		REIMS Q-TOF	42 lipid metabolites were tentatively identified and 12 out of 13 lipid biomarkers showed higher intensities in GBM	Ma et al., 2021

14 recurrent GBMs post anti-angiogenic therapy: (7 responders and 7 not responders)	FFPE	Quantification of 4957 unique proteins (269 different proteomic patterns between responders and non-responders); TMEM173 and FADD may be used to predict the response to anti-angiogenic therapy and prognosis before recurrence	LC-MS	To identify novel prognostic biomarkers that can predict the therapeutic response to anti-angiogenic agents in patients with recurrent glioblastoma	Jeon et al., 2023
36 GBM IDH-WT	Plasma	Characterize the plasma levels of biogenic amines in GBM patients before and after surgery, as well as before and after concurrent chemoradiation.	LC-MS TripleTOF 6600	Surgery was associated with increased levels of 12 metabolites and decreased levels of 11 metabolites; Chemoradiation was associated with increased levels of three metabolites and decreased levels of three other metabolites	Aboud et al., 2023
46 GBMs; 30 samples by SpiderMass	FF	Total of 4936 proteins were identified, of which 1183 proteins showed a significant difference in expression between the three groups	MALDI-MSI SpiderMass Ultraflex II MALDI-TOF	Three molecular groups associated with immune, neurogenesis, and tumorigenesis signatures with high intra-tumoral heterogeneity;	Duhamel et al., 2022

Table 2. The immunopeptidome analysis in glioblastoma samples

Source biological material	Sampling	Identified immunopeptidome	Instrumentation	Author
Stage IV glioma tissues; T2, U118 and K562 cell lines	Peptides were isolated using HLA-specific antibodies; antibody BB7.2 was used for isolation of HLA-A*02 peptides	Identified 6820 HLA-restricted peptides, comprising 3686 different HLA-A*02-restricted sequences eluted with the HLA-A*02-specific BB7.2 antibody	NanoLC-LTQ Orbitrap	Dutoit et al., 2012
Peripheral blood (PB) and tumour tissues samples from GBM patients	HLA I peptides were isolated with W6/32 mAb bound to AminoLink beads	22,583 different HLA peptides were identified from tumour; 26,841 different HLA peptides were identified from plasma	Nano Ultimate 3000 RSLC-Q Exactive Plus	Shraibman et al., 2019
Six DIPG patient-derived cell lines	BB7.2 column was used to capture HLA-A*02:01 peptides; W6/32 column was used to capture remaining HLA class I peptides; GAPA3 antibody to immunoprecipitate the HLA-A3 peptide complexes	7,459 HLA-A*02:01–restricted peptides; 2,115 restricted peptides identified from HLA-A3+ cell line; 16,542 peptides were identified with W6/32	Nano-Ultimate 3000 UHPLC-Q-Exactive Plus or Tribrid Fusion	Pandey et al., 2023
Glioblastoma stem-like cells; peripheral blood mononuclear cells	In-house produced mAb W6/32 for isolation of HLA I; in-house produced HLA-DR-specific antibody L243 and pan-HLA class II-specific antibody Tü39 for isolation of HLA II	GBM tissue samples yielded 46,429 HLA I peptides and 1877HLA II peptides; GSC yielded 4863 HLA I peptides and 1321 HLA II peptides	Nano Ultimate 3000-LTQ Orbitrap XL or Orbitrap Fusion	Neidert et al., 2018

Figure captions:

Scheme 1. Illustration of mass spectrometry based techniques used in the analysis of different classes of molecules in the studies of glioblastoma. Electrospray ionization (ESI); Desorption electrospray ionization (DESI); Matrix-assisted laser desorption/ionization (MALDI); Surface-enhanced laser desorption/ionization (SELDI).

Figure 1. Use of DIA acquisition methods in neuroproteomics. Described studies have used DIA-MS for the quantification of the brain proteome (purple) and advances in DIA which allowed higher throughput and improved databases and libraries (green). Taken and adapted from (Li et al., 2020)

Figure 2. Double immunofluorescence staining of BTK with various biomarkers in GBM FFPE sections. (A) BTK was stained with SOX2, a cancer stem marker. (B) BTK stained with CD163, M2-like macrophage marker. (C) BTK stained with CD68, a pan-macrophage marker. The figure demonstrates that BTK, a tyrosine-protein kinase implicated in blood malignancies was found to be expressed in various cell types (cancer stem cells and/or macrophages) but was notably absent in all GBM cell lines models, as observation in GBM kinome data (Al Shboul et al., 2021). Figure adapted form (Al Shboul et al., 2021).

Figure 3. (A) Time course and workflow of patient care associated with a typical 5-h neurosurgery in the AMIGO, MRI-equipped, operative suite at Brigham and Women's Hospital. (B) Negative ion mode DESI mass spectra obtained using an amaZon Speed ion trap from m/z 130–165 (Bruker Daltonics) from a swab (Left), a smear (Center), and a section (Right) for sample S72. (C) Normalized 2-HG signal is represented with a warm color scale as indicated by the scale bar, set from the lowest (yellow) to highest (orange) levels detected from this individual case. Stereotactic positions were digitally registered to the preoperative MRI using neuro navigation (BrainLab system) in a standard operating room. The 3D tumour volume is shown (Upper). Classification results of samples S74, S72, S73, and S71 are further visualized on axial sections (Lower). (Figure included with permission from Santagata et al., 2014) (Santagata et al., 2014)

Figure 4. Brain proliferation zones and MALDI-IMS clustering comparison. Representative images of IF and MALDI-IMS for both healthy and tumour treated and non-treated are shown. Healthy brain and GBM biopsy sections were prepared after incubating fresh biopsies in DMSO (vehicle) or TMZ (10 mg/mL, 4 h) and analyzed by MALDI-IMS at 50–100 μm lateral resolution. Brain proliferation zones were determined by MKI67+ IF staining and used to select the MALDI-IMS cluster, generated by HD-RCA from consecutive tissue sections (Garate et al., 2020). HD-RCA clustering enabled the identification of the IMS regions of interest (Cluster*) with greater correlation (evaluated by direct visual inspection) with the MKI67+ IFs, based on the similarity of lipidomic content in each MALDI-IMS experiment. Proliferation zones are marked in orange in MKI67+ IFs. DAPI was used as a nucleus marker (marked in blue on IF MKI67 images). The distribution of PI 38:4 (885.55 m/z) is shown as a representative MALDI-IMS lipid distribution. Color scale indicates the intensity of the PI 38:4 -H distribution (0, black; 1, white). HD-RCA number of segments was set from 2 to 5, with prior background noise filtration using in-house MATLAB algorithms (Garate et al., 2020). (Taken with permission from Maimó-Barceló et al.) (Maimo-Barcelo et al., 2022)

Scheme 1.

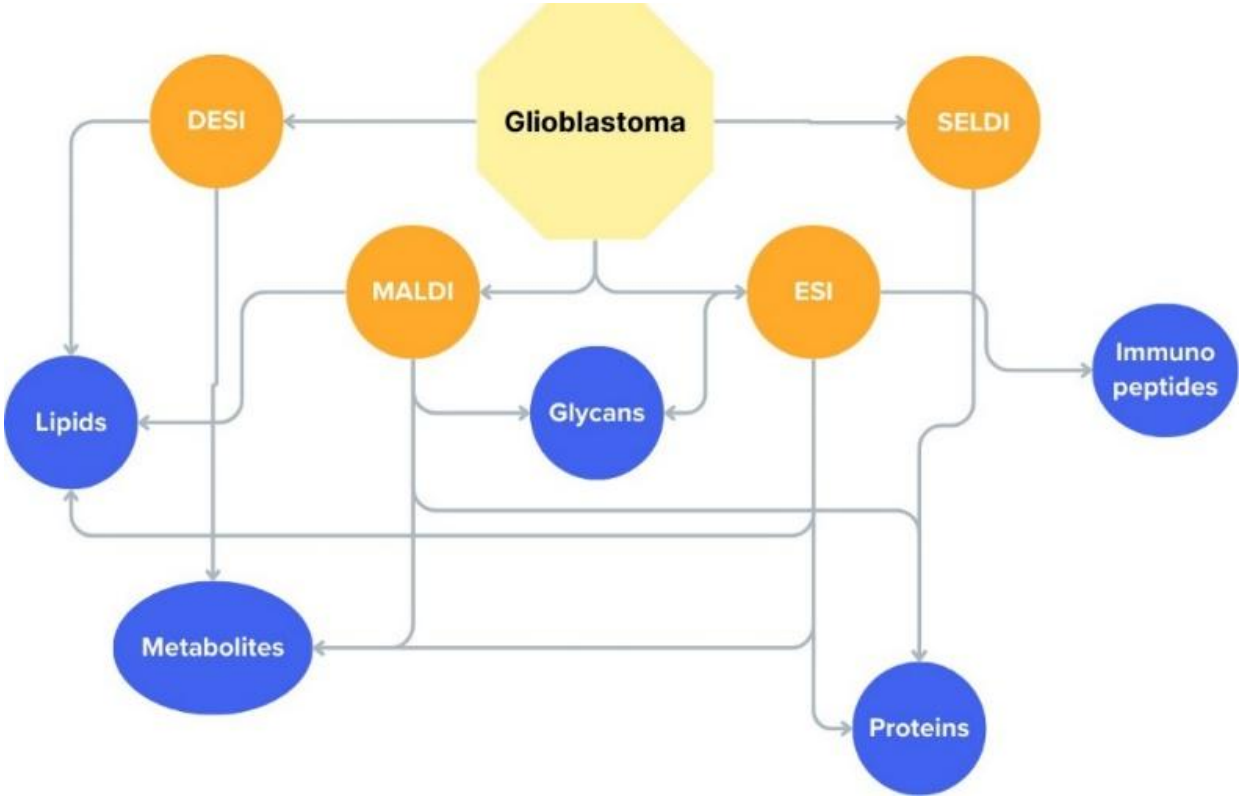
Glioblastoma
DESI
SELDI
MALDI
ESI
Lipids
Glycans
Immuno peptides
Metabolites
Proteins

Figure 1.

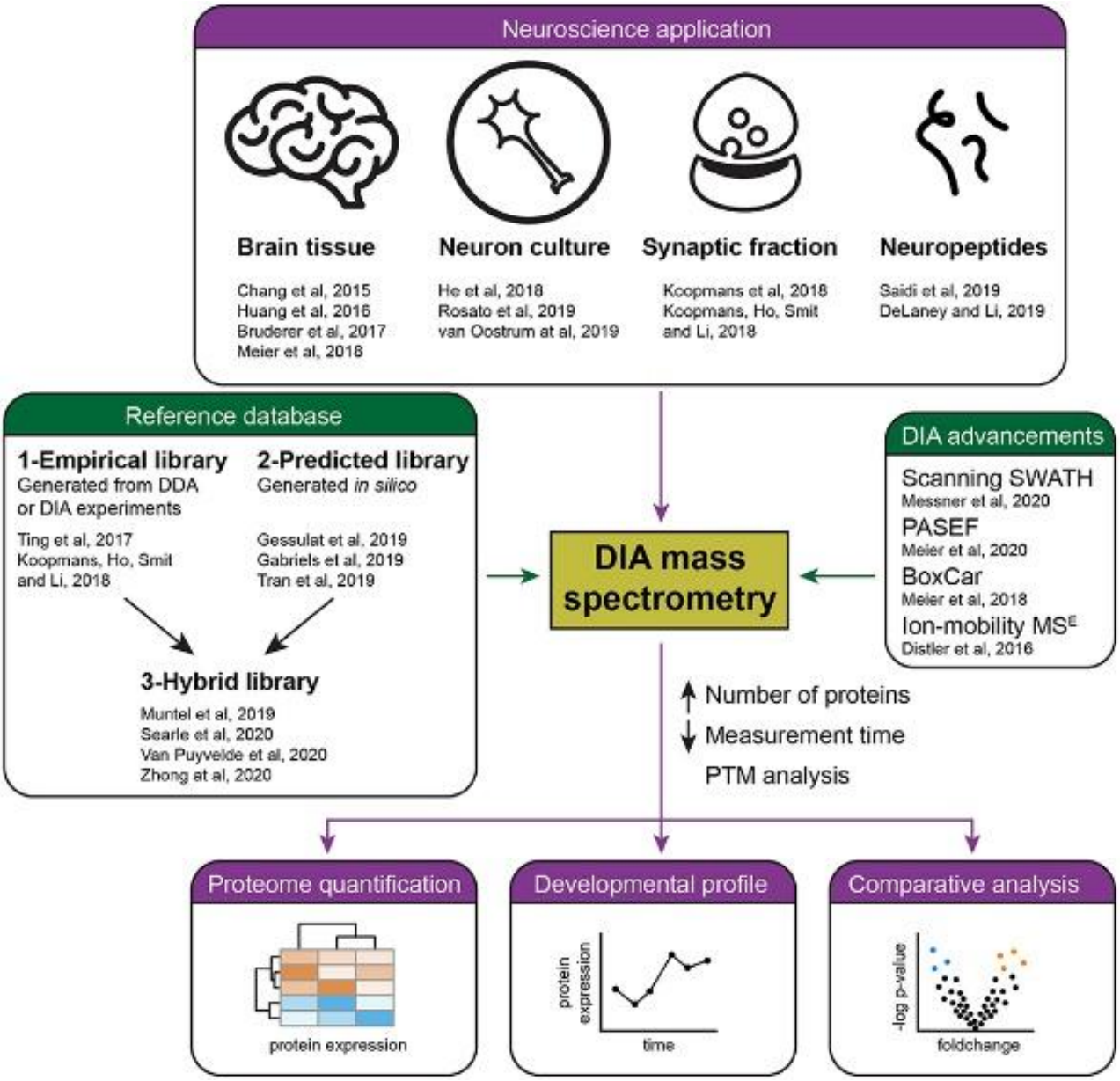
Neuroscience application
Brain tissue
Chang et al, 2015
Huang et al, 2016
Bruderer et al, 2017
Meier et al, 2018
Neuron culture
He et al, 2018
Rosato et al, 2019
van Oostrum et al, 2019
Synaptic fraction
Koopmans et al, 2018
Koopmans, Ho, Smit and Li, 2018
Neuropeptides
Saidi et al, 2019
DeLaney and Li, 2019
Reference database
1-Empirical library
Generated from DDA or DIA experiments
Ting et al, 2017
Koopmans, Ho, Smit and Li, 2018
2-Predicted library
Generated in silico
Gessulat et al, 2019
Gabriels et al, 2019
Tran et al, 2019
3-Hybrid library
Muntel et al, 2019
Searle et al, 2020
Van Puyvelde et al, 2020
Zhong et al, 2020
DIA mass spectrometry
DIA advancements
Scanning SWATH
Messner et al, 2020
PASEF
Meier et al, 2020
BoxCar
Meier et al, 2018
Ion-mobility MSE
Distler et al, 2016
Number of proteins
Measurement time
PTM analysis
Proteome quantification
protein expression
Developmental profile
protein expression
time
Comparative analysis
-log p-value
foldchange

Figure 2.

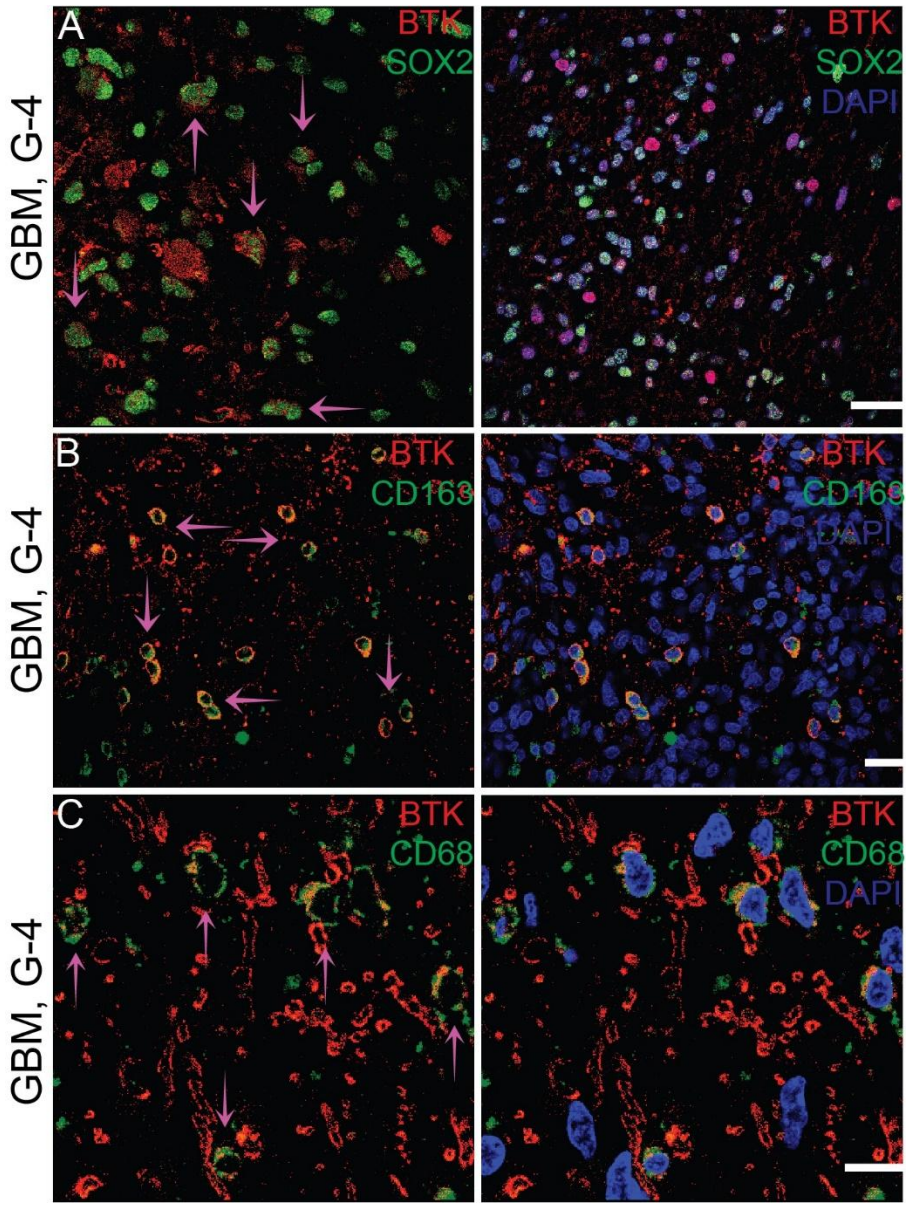
A
BTK
SOX2
BTK
SOX2
DAPI
GBM, G-4
B
BTK
CD163
BTK
CD163
DAPI
GBM, G-4
C
BTK
CD68
BTK
CD68
DAPI
GBM, G-4

Figure3.

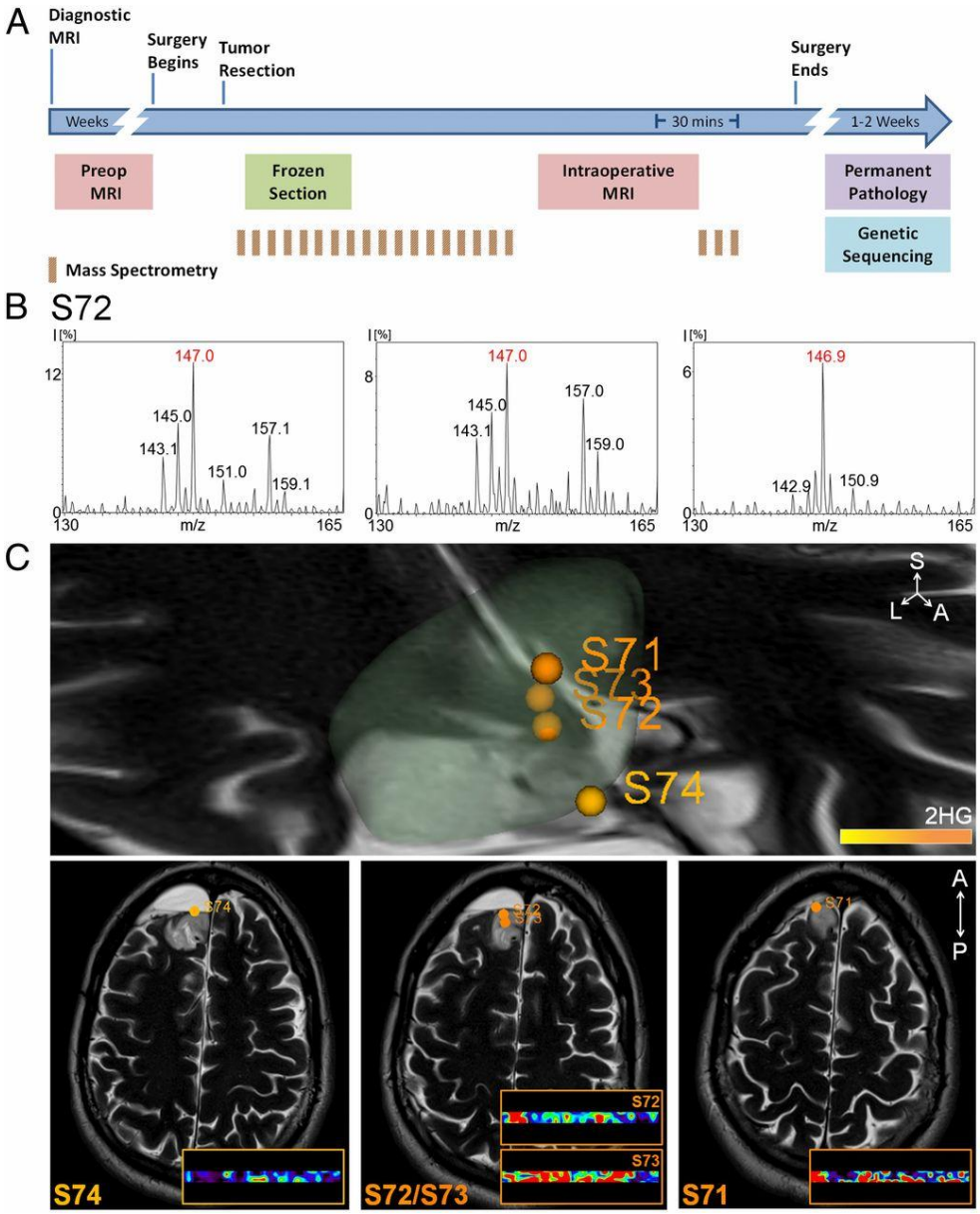
A
Diagnostic MRI
Surgery Begins
Tumor Resection
Surgery Ends
Weeks
30 mins
1-2 Weeks
Preop MRI
Frozen Section
Intraoperative MRI
Permanent Pathology
Genetic Sequencing
Mass Spectrometry
B S72
[%]
147.0
145.0
143.1
157.1
151.0
159.1
147.0
145.0
143.1
157.0
159.0
146.9
142.9
150.9
130
m/z
165
C
S
L
A
S71
S73
S72
S74
2HG
A
P
S74
S72/S73
S71
S72
S73

Figure 4.

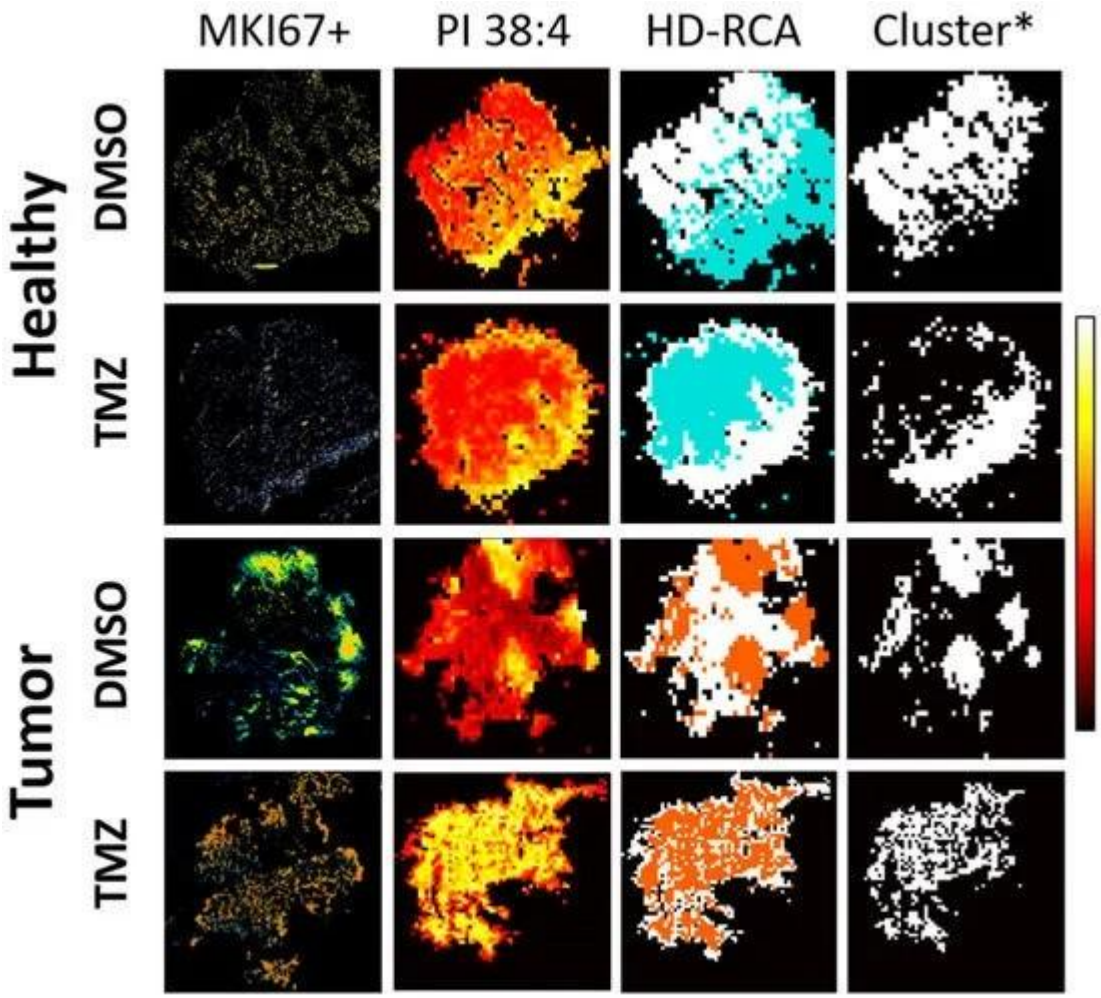

List of acronyms

Acronym	Meaning
2HG	2-hydroxyglutarate
ACN	Acetonitrile
AEG-1	Astrocyte elevated gene-1
AHNAK	neuroblast differentiation-associated protein
AHNAK	neuroblast differentiation-associated protein
AKT2	Protein kinase B
Ang2	Angiopoietin-2
APOA4	Apolipoprotein A-IV
APOB	Apolipoprotein B
APOE	Lectin-like oxidized LDL receptor 1
APOE	Apolipoprotein E
APPM	Atmospheric pressure photoionization mass spectrometry
ATRA	all-trans retinoic acid
BM-hMSCs	bone marrow-derived human mesenchymal stem cells
BTK	Bruton's tyrosine kinase
C9	Complement component 9
CAFs	Cancer-associated fibroblasts
CAMK2D	calcium/calmodulin-dependent protein kinase type II subunit delta
CAMK2D	Calcium/calmodulin-dependent protein kinase II delta
CD163	Cluster of differentiation 163
CD44	Cluster of differentiation 44
CD47	Cluster of differentiation 47
CD68	Cluster of differentiation 68
CD74	Cluster of differentiation 74
CDK1	Cyclin-dependent kinase 1
CDKN2A/B	Cyclin-dependent kinase inhibitor 2A/B
Cer	ceramide
CERU	Ceruloplasmin
CFL1	Cofilin-1
CID	Collision-induced dissociation
CLIC4	Chloride intracellular channel protein 4
CLIC4	Chloride intracellular channel protein 4
CNS	Central nervous system
CPB2	Carboxypeptidase B2
CRP	C-reactive protein
CSF	Cerebrospinal fluid
CTAs	cancer-testis antigens
CXCR2	C-X-C chemokine receptor type 2
CXCR4	C-X-C chemokine receptor type 4
Cyr61/CCN1	Cysteine-rich angiogenic inducer 61

DAPI	4',6-diamidino-2-phenylindole
DDA	Data-dependent acquisition
DDT	D-Dopachrome Tautomerase
DESI-MS	Desorption electrospray ionization mass spectrometry
DESI-MSI	Desorption electrospray ionization mass spectrometry imaging
DIA	Data-independent acquisition
DIPG	diffuse intrinsic pontine glioma
DMF	Dimethyl fumarate
DYRK1A	Dual-specificity tyrosine-regulated kinase 1A
EGFR	Epidermal growth factor receptor
EIF4B	Eukaryotic translation initiation factor 4B
ER	Endoplasmic reticulum
ERK	Extracellular signal-regulated kinase
Eta-1	Ectopic thyroid-associated protein 1
extrachromosomal DNA	ecDNA
FAS	Fatty acid synthase
Fe-NTA	Iron-Nitrilotriacetic Acid
FF	Frozen fresh
FFPE	Formalin-fixed paraffin-embedded
FGF-b	Fibroblast growth factor-basic
FKBP5	FK506-binding protein 5
FKBP5	peptidyl-prolyl *cis*-trans isomerase
GBM	glioblastoma
GFAP	Glial fibrillary acidic protein
GSN	Gelsolin
H2B	Histone H2B
HCD	Higher-energy collisional dissociation
HRG	Histidine-rich glycoprotein
HRG	Histidine-rich glycoprotein
IDH	Isocitrate dehydrogenase
IFNA	Interferon-alpha
IGFBP-2	Insulin-like growth factor-binding protein 2
IGHA1	Immunoglobulin heavy constant alpha 1
IGKC	Immunoglobulin kappa constant
IGKC	Ig kappa chain C region
IMAC	Immobilized metal ion affinity chromatography
ITGB2	Integrin beta-2
ITGB3	integrin β3
iTRAQ	Isobaric tags for relative and absolute quantitation
KNG1	Kininogen-1
LCM	Laser capture microdissection
LCN2	lipocalin 2
LDHA	Lactate dehydrogenase A

LEG1	Lectin-like oxidized LDL receptor 1
LEG1	Galectin-1 LGALS1
LRG1	Leucine-rich alpha-2-glycoprotein 1
MALDI	Matrix-assisted laser desorption/ionization
MALDI-FTICR	Matrix-assisted laser desorption/ionization Fourier-transform ion cyclotron resonance
MALDI-TOF	Matrix-assisted laser desorption/ionization time-of-flight
mammalian target of rapamycin	mTOR
MAPK	Mitogen-activated protein kinase
MAPS	4-maleicanhydridoproton sponge
MAPT	Microtubule-associated protein tau
MET	Mesenchymal-epithelial transition factor
MGMT	O-6-methylguanine-DNA methyltransferase
MIF	Macrophage migration inhibitory factor
MMP-2	Matrix metalloproteinase-2
MMP-9	Matrix metalloproteinase-9
MRS	Magnetic resonance spectroscopy
MS	Mass spectrometry
NEFM	Neurofilament medium polypeptide
NOTCH3	Neurogenic locus notch homolog protein 3
NP1L1	Neuropilin-1-like protein 1
NP1L1	Nucleosome assembly protein 1-like 1
OAS2	2'-5'-Oligoadenylate Synthase 2
OLIG2	Oligodendrocyte transcription factor 2
OPN	Osteopontin
PC	phosphatidyl- choline
PC	glycerophosphocholines
PDGFR	Platelet-derived growth factor receptor
PDGFR	Serine protease inhibitor
PDGFRA	Platelet-derived growth factor receptor alpha
PDIA1	Protein disulfide-isomerase P4HB
PDX	Patient-derived xenograft
PE	phosphatidylethanolamine
PET	Positron emission tomography
phosphatase and tensin homolog	PTEN
Phosphatidylinositol-4,5-Bisphosphate 3-Kinase Catalytic Subunit Alpha	PIK3CA
PI	phosphatidylinositol
PI3K	Phosphatidylinositol 3-kinase
PIRL-MS	Phospholipid isomer-based lipidomics mass spectrometry
PLC	Phospholipase C
PLCG1	Phospholipase C gamma 1
PNA	Peanut agglutinin
Poly-ICLC	polyinosinic-polycytidylic acid stabilized with polylysine and carboxymethylcellulose

protein kinase B	AKT
PS	phosphatidylserine
PTEN	Phosphatase and tensin homolog
PTPN11	Protein tyrosine phosphatase non-receptor type 11
PTPRJ1	Protein tyrosine phosphatase receptor type J
PVDF	Polyvinylidene difluoride
QTRAP	Quadrupole ion trap
RB1	Retinoblastoma 1
REIMS	Rapid evaporative ionization mass spectrometry
RPLC	Reversed-phase liquid chromatography
S100A8	S100 Calcium Binding Protein A8
S100A9	S100 Calcium Binding Protein A9
SELDI-TOF-MS	Surface-enhanced laser desorption/ionization time-of-flight mass spectrometry
SERPH	Serpin H1 SERPINH1
SERPINA3	Serpin family A member 3
SLC1A5	Solute carrier family 1 member 5
SM	sphingomyelin
SMARCC2	SWI/SNF-related matrix-associated actin-dependent regulator of chromatin subfamily C member 2
SOX2	SRY (sex-determining region Y)-box 2
SPB	sodium phenylbutyrate
SPP1	Secreted phosphoprotein 1
SREBP1	Sterol regulatory element-binding protein 1
SRM	Selected reaction monitoring
SRSF3	Serine/arginine-rich splicing factor 3
ST	sulfatide
STMN1	Stathmin 1
TAAs	tumour-associated antigens
TAGL2	Triacylglycerol lipase 2
TAGL2	transgelin-2
TAMs	Tumor-associated macrophages
TENA	Tenascin TNC
TERT	Telomerase reverse transcriptase
TFA	trifluoroacetic acid
TKA	Trichosanthes kirilowii agglutinin
TMZ	Temozolomide
TNC	Tenascin-C
TSP1/2	Thrombospondin 1/2
TTYH1	Tweety homolog 1
VEGF	Vascular endothelial growth factor
VIM	Vimentin
VTNC	Vitronectin
WHO	World Health Organization

YES	Tyrosine-protein kinase Yes
YKL40	Chitinase-3-like protein 1